

## RESEARCH ARTICLE

# Integration of celestial compass cues in the central complex of the locust brain

Uta Pegel<sup>1</sup>, Keram Pfeiffer<sup>2</sup> and Uwe Homberg<sup>1,\*</sup>

## ABSTRACT

Many insects rely on celestial compass cues such as the polarization pattern of the sky for spatial orientation. In the desert locust, the central complex (CX) houses multiple sets of neurons, sensitive to the oscillation plane of polarized light and thus probably acts as an internal polarization compass. We investigated whether other sky compass cues like direct sunlight or the chromatic gradient of the sky might contribute to this compass. We recorded from polarization-sensitive CX neurons while an unpolarized green or ultraviolet light spot was moved around the head of the animal. All types of neuron that were sensitive to the plane of polarization (*E*-vector) above the animal also responded to the unpolarized light spots in an azimuth-dependent way. The tuning to the unpolarized light spots was independent of wavelength, suggesting that the neurons encode solar azimuth based on direct sunlight and not on the sky chromatic gradient. Two cell types represented the natural 90 deg relationship between solar azimuth and zenithal *E*-vector orientation, providing evidence to suggest that solar azimuth information supports the internal polarization compass. Most neurons showed advances in their tuning to the *E*-vector and the unpolarized light spots dependent on rotation direction, consistent with anticipatory signaling. The amplitude of responses and its variability were dependent on the level of background firing, possibly indicating different internal states. The integration of polarization and solar azimuth information strongly suggests that besides the polarization pattern of the sky, direct sunlight might be an important cue for sky compass navigation in the locust.

**KEY WORDS:** Insect brain, Desert locust, Head direction cells, Spatial orientation, Sky compass, Chromatic gradient

## INTRODUCTION


For navigation, defined as the ability to reach a desired goal, many animals rely on visual cues, such as landmarks and sky compass signals. Whereas the presence of landmarks depends on the structure of the habitat, sky compass signals are available almost everywhere, and thus represent highly reliable navigational cues (Gould, 1998; Frost and Mouritsen, 2006). Features of the sky providing navigational information include its polarization pattern, its chromatic gradient, and the position of the sun. By scattering at

air molecules unpolarized sunlight becomes partly linearly polarized (Rossel, 1993; Wehner, 2001). The electric field vectors (*E*-vectors) in the sky are arranged tangentially along concentric circles around the sun (Fig. 1), and thus reference solar/antisolar position (Rossel et al., 1978; Rossel, 1993). The percentage of polarization increases from the solar and antisolar position to a maximum at an angle 90 deg from the sun (Fig. 1A). In contrast, the chromatic gradient arises from an intensity gradient of long wavelength light and a uniform distribution of short wavelength light across the sky (Fig. 1A). The resulting color contrast is high at the solar position and low at the antisolar point (Coemans et al., 1994). It allows for distinction between the solar and the antisolar hemisphere, especially at low solar elevations, when the polarization pattern is ambiguous.

Sky compass navigation has been demonstrated in several insect species, including bees (von Frisch, 1949; Brines and Gould, 1979), ants (Wehner and Müller, 2006), locusts (Kennedy, 1951), monarch butterflies (Reppert et al., 2004; Stalleicken et al., 2005), dung beetles (Dacke et al., 2003; el Jundi et al., 2014b), and fruit flies (Weir and Dickinson, 2012). All of these animals possess a region of the compound eye containing specialized homochromatic photoreceptors, the dorsal rim area (DRA), which serves as a polarization detector (Labhart and Meyer, 1999). In contrast, chromatic signals are perceived by photoreceptors in the main retina with different spectral sensitivities enabling color vision (Wernet et al., 2015). In the locust, intracellular recordings showed that polarization-sensitive neurons of the medulla and anterior optic tubercle (AOTU) integrate polarized and chromatic light information by responding to unpolarized chromatic stimuli in an azimuth-dependent way (Kinoshita et al., 2007; Pfeiffer and Homberg, 2007; el Jundi et al., 2011). Neurons of the AOTU are connected to neurons of the central complex (CX), a group of neuropils spanning the midline of the brain. In fruit flies several studies revealed the importance of the CX for navigational tasks (Neuser et al., 2008; Ofstad et al., 2011; Seelig and Jayaraman, 2015; Weir and Dickinson, 2015). A prominent role of the CX in sky compass signaling has been demonstrated in monarch butterflies (Heinze and Reppert, 2011), dung beetles (el Jundi et al., 2015), crickets (Sakura et al., 2008) and desert locusts (Homberg et al., 2011). In monarchs and dung beetles, CX neurons are sensitive to plane polarized light and the azimuth of unpolarized chromatic cues. The processing of polarized light signals has been studied most extensively in neurons of the locust CX (Heinze and Homberg, 2007; Bech et al., 2014; Bockhorst and Homberg, 2015), but little is known about their coding of other sky compass cues (el Jundi et al., 2014a). In order to uncover the role of direct sunlight and chromatic information in sky compass signaling in the locust, we studied the processing of chromatic cues in comparison with the processing of polarized light signals, using intracellular recordings from a variety of CX neurons.

<sup>1</sup>Animal Physiology, Department of Biology, Philipps-University, Karl-von-Frisch-Straße 8, 35032 Marburg, Germany. <sup>2</sup>Behavioral Physiology and Sociobiology (Zoology II), Biozentrum, University of Würzburg, Am Hubland, 97074 Würzburg, Germany.

\*Author for correspondence (homberg@biologie.uni-marburg.de)

 K.P., 0000-0001-5348-2304; U.H., 0000-0002-8229-7236

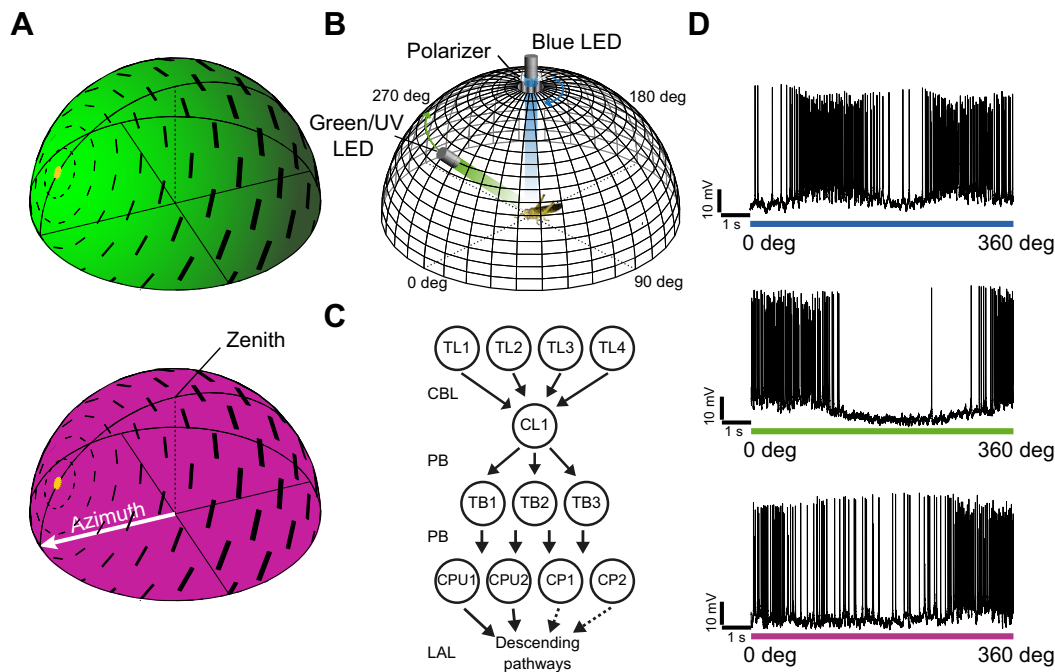


**Fig. 1. Compass cues of the sky and visual stimulation.** (A) Schematic illustration of the polarization pattern and the spectral gradient in the sky. Electric field vectors (black bars) are arranged tangentially along concentric circles around the sun. The degree of polarization, indicated by the thickness of the bars, increases from the sun towards a 90 deg angle and decreases again towards the antisolar point. The chromatic gradient is the product of a long-wavelength light intensity gradient (green) and a uniform distribution of short-wavelength light (purple), resulting in a high color contrast near the sun and a lower color contrast near the antisolar point. The solar azimuth, indicating the horizontal direction of the sun, and the zenith, the point in the sky vertically above the observer, are labelled. (B) Visual stimulation. The light of a blue LED passed a rotating polarizer in the zenith. A green (or UV) LED rotated at an elevation of 45 deg around the head of the animal to produce an unpolarized light stimulus. (C) Schematic illustration of information flow in the CX. Circles represent neuron types. Arrows indicate the suggested direction of connectivity between neurons. Because varicose arborizations of CP1 and CP2 neurons are confined to small areas in the lateral accessory lobe (LAL) their contacts to descending neurons are hypothetical and shown as dotted lines. (D) Spike train from TL2 neuron shown in Fig. 2B during a 360 deg clockwise rotation of the zenithal polarizer (top panel), the green light spot (middle panel) and the UV light spot (bottom panel). CBL, central body lower division; PB, protocerebral bridge; CL1, columnar neuron of the CBL type 1; CP1/2, columnar neuron of the PB type 1/2; CPU1/2, columnar neuron of the PB and central body upper division type 1/2; TB1/2/3, tangential neuron of the PB type 1/2/3; TL1/2/3/4, tangential neuron of the CBL type 1/2/3/4.

## MATERIALS AND METHODS

### Animals and preparation

Desert locusts (*Schistocerca gregaria* Forsskål 1775) were reared under crowded conditions either in the laboratory at 28°C under a 12 h:12 h light:dark cycle or during summer in a greenhouse. Experiments were performed on sexually mature animals at least one week after final moult. Animals were mounted onto a metal holder using dental wax. Wings and legs were cut off, and the mouthparts were immobilized by wax. The head capsule was opened anteriorly, and fat tissue and tracheal air sacs were removed. Muscles close to the brain as well as the esophagus were transected, and the gut was removed through an abdominal incision in order to reduce brain movements. Hemolymph leakage was prevented using a thread to tie off the abdomen. To further stabilize the brain, it was supported from the posterior by a small metal wire platform. To ease electrode penetration the neural sheath above the central brain was removed using forceps. During animal preparation and intracellular recording the brain was immersed in locust saline (Clements and May, 1974) containing 0.09 mol l<sup>-1</sup> saccharose.

### Electrophysiology and visual stimulation

For intracellular recordings sharp glass microelectrodes were drawn from borosilicate capillaries (Hilgenberg, Malsfeld, Germany) using a Flaming/Brown horizontal puller (P-97, Sutter Instrument Company, Novato, CA, USA). The electrode tip was filled with 4% Neurobiotin (Vector Laboratories, Burlingame, CA, USA) diluted in 1 mol l<sup>-1</sup> KCl, and the electrode shank with 1 mol l<sup>-1</sup> KCl.

Neural signals were amplified 10× with a custom-built amplifier and visualized with an oscilloscope (DS 1052Eh, Rigol Technologies, Beijing, China). A digitizer (CED1401plus, Cambridge Electronic Design, Cambridge, UK) was used to sample the signals at a rate of 20 kHz. The data were stored on a PC using Spike2 (version 6.022, Cambridge Electronic Design). After the recording Neurobiotin was injected into the neuron by applying constant positive current of about 1 nA for 3–4 min. During the recording the animal's body axis was oriented vertically with its head uppermost (Pfeiffer et al., 2005). The locust was stimulated with polarized blue light, generated by a blue light emitting diode (LED; Oslon SSL 80, LDCQ7P, 452 nm, Osram Opto Semiconductors, Regensburg, Germany, or LXML-PR01-0500, 447.5 nm, Philips Lumileds Lighting Company, San José, CA, USA). Light intensity was adjusted to a photon flux of 1.7×10<sup>13</sup> photons cm<sup>-2</sup> s<sup>-1</sup>. The LED was positioned in the zenith (visual angle 32.5 or 18.6 deg). Its light passed through a diffusor and a polarizer (HNP'B, Polaroid, Cambridge, MA, USA), which rotated 360 deg clockwise or counterclockwise, with 40 or 36 deg s<sup>-1</sup> velocity. A stimulation velocity of 30 deg s<sup>-1</sup> was used in four experiments. In addition, we stimulated the animal with unpolarized green and ultraviolet (UV) light spots. The green light spot was generated by a green LED (LED535-series, 535 nm, Roithner Lasertechnik, Vienna, Austria, or Oslon SSL 80, LT CP7P, 528 nm, Osram Opto Semiconductors; photon flux adjusted to 10<sup>14</sup> photons cm<sup>-2</sup> s<sup>-1</sup>), and the UV light spot by an ultraviolet LED (XSL-355-5E, 355 nm, Roithner Lasertechnik, or Nichia STS-DA1-2394D, NCSU033B(T),

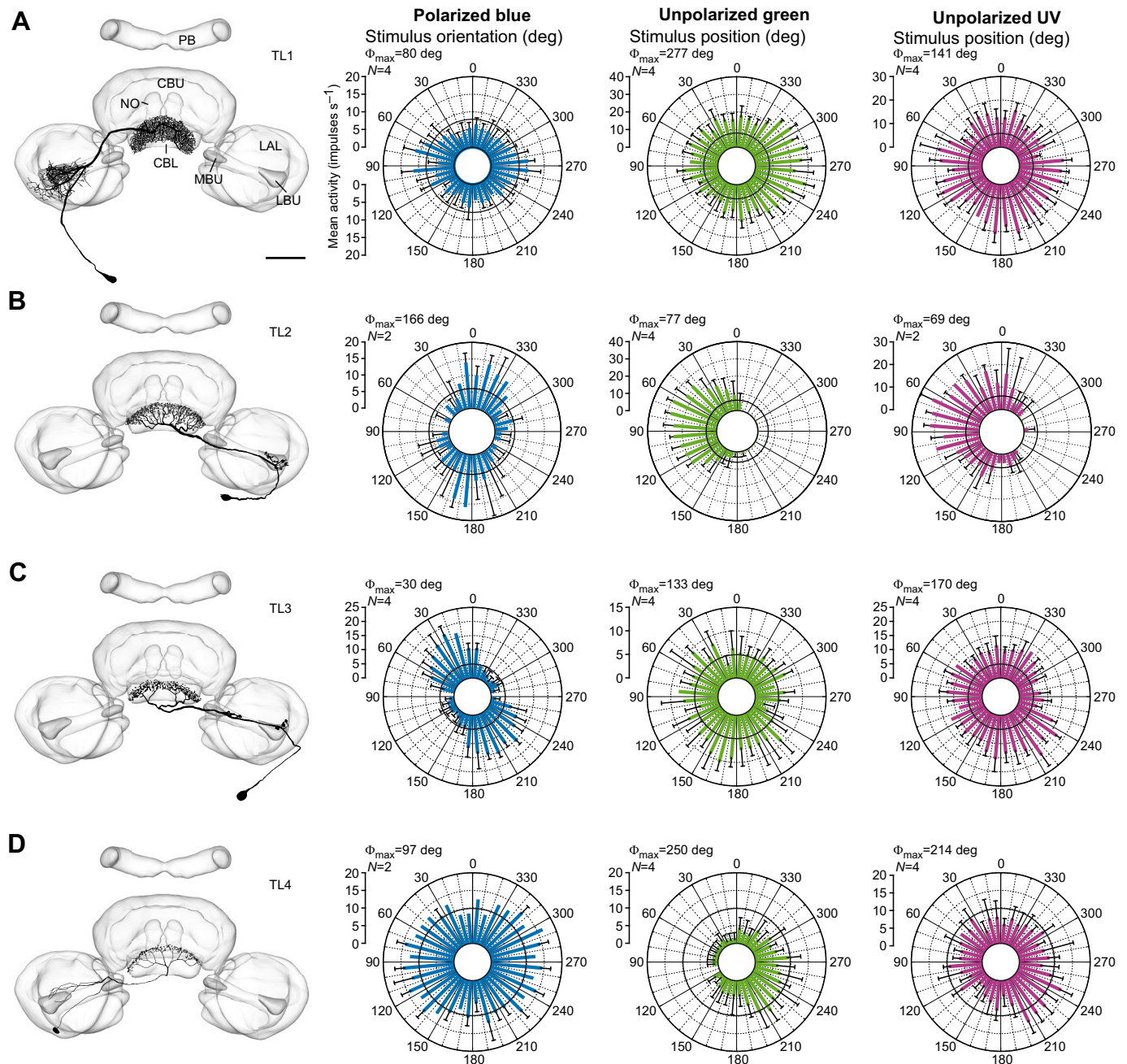


**Fig. 2. Morphology and physiology of tangential neurons of the lower division of the central body (TL) of the desert locust *Schistocerca gregaria*.** (A–D) Reconstructions of a TL1, TL2, TL3 and TL4 neuron, respectively, projected onto the standard CX (el Jundi et al., 2010; posterior view; left-hand panels) and circular histograms of stimulus responses (right-hand panels) from the animals' perspective.  $N$  responses to 360 deg rotations of the polarizer (polarized, blue), a green and a UV light spot (unpolarized green, unpolarized UV) were pooled and plotted as means in 10 deg bins. Black circles indicate median background activity. Error bars indicate s.d. The preferred  $E$ -vector orientation or azimuth of the unpolarized light spots is indicated by  $\Phi_{\max}$ . Scale bar, 100  $\mu\text{m}$ . CBL, central body lower division; CBU, central body upper division; LAL, lateral accessory lobe; LBU, lateral bulb; MBU, medial bulb; NO, noduli; PB, protocerebral bridge.

365 nm, Nichia Corporation, Anan, Japan; photon flux adjusted to  $10^{14}$  photons  $\text{cm}^{-2} \text{s}^{-1}$ ). Their light passed through a diffusor. The unpolarized light stimuli covered a visual angle of 16.3 deg. They were moved around the head of the animal at an elevation of 45 deg and a velocity of 40 or 36  $\text{deg s}^{-1}$  (Fig. 1B).

### Histology

Brains were dissected in locust saline and immersed overnight at 4°C in fixative containing 4% paraformaldehyde, 0.25% glutaraldehyde and 0.2% saturated picric acid in 0.1  $\text{mol l}^{-1}$

phosphate-buffered saline (PBS). They were stored for up to 14 days in sodium phosphate buffer at 4°C. Brains were rinsed 4×15 min in 0.1  $\text{mol l}^{-1}$  PBS and incubated for 3 days in Cy3-conjugated streptavidin (Dianova, Hamburg, Germany) diluted 1:1000 in 0.1  $\text{mol l}^{-1}$  PBS containing 0.3% Triton X-100 (PBT) at 4°C in the dark. After incubation they were rinsed 2× in 0.1  $\text{mol l}^{-1}$  PBT and 3× in 0.1  $\text{mol l}^{-1}$  PBS for 30 min each, dehydrated in an increasing ethanol series (30, 50, 70, 90, 95 and 100% for 15 min each), cleared in a 1:1 mixture of 100% ethanol and methyl salicylate (Merck, Darmstadt, Germany) for 20 min, followed by



pure methyl salicylate for 1 h, and were finally mounted in Permout (Fisher Scientific, Waltham, MA, USA) between two coverslips. Neurons were visualized using a confocal laser scanning microscope (Leica TCS-SP5, Leica Microsystems, Wetzlar, Germany) with a DPSS Laser (561 nm) and AMIRA (version 5.4.5, FEI Visualization Science Group, Mérignac cedex, France). Neurons were reconstructed two-dimensionally using Adobe Photoshop CC (version 2014.2.1, Adobe Systems, San José, CA, USA).

### Data pre-processing

Physiological data were evaluated only from recordings of neurons that were clearly identified by means of their labeling. Recordings were pre-processed using Spike2 (Cambridge Electronic Design). The quality of recording was determined by visual inspection. Recordings with strong fluctuations in baseline or with low spike amplitudes (<5 mV) were rejected. In the selected recordings, spikes were detected with threshold-based event detection in Spike2. The data were then exported as a mat-file. All subsequent analysis was performed using MATLAB (version 2016a, The MathWorks, Natick, MA, USA).

### Background activity

To analyse neuronal responses during polarizer/light spot rotation we calculated the background activity (BA) of each neuron. Only stable parts of the recording during absence of stimulation or current injection were selected. Spikes were binned in 1 s bins. Spike counts of all bins were used to calculate the median, the lower and upper quartile as well as the 2.5th and 97.5th percentile of BA. To assess the role of BA we analysed responses of neurons with high and low BA separately. A cell type-specific median BA was calculated out of all median BAs of the neurons belonging to that cell type. Median individual BAs lower than or equal to the cell type-specific median BA were defined as low BA, whereas median individual BAs higher than the cell type-specific BA were defined as high BA.

### Stimulus responsiveness

For each stimulus presentation (i.e. 360 deg rotation of *E*-vector/light spot) the neuron's stimulus–response curve was obtained by calculating the spike rate within each of 36 bins of 10 deg. From the stimulus–response curves we tested the responses for unidirectionality (green/UV spot stimulus) by angular-linear correlation analysis (Zar, 1999; Berens, 2009). The angles of bin centers were used as the angular variable and the mean spiking activity in each bin as the linear variable. The responses to the rotating *E*-vector were tested for bidirectionality, thus the angular variable was doubled (Batschelet, 1981). The criterion for responsiveness to the plane of polarized light or the azimuth of unpolarized light spots was the significance of the resulting correlation coefficient  $r_{al}$  ( $\alpha=0.05$ ).

### Stimulus–response characteristics

Spike times were transformed into angles (hereafter referred to as spike angles) by multiplying them with the rotation velocity of the stimulus. In the case of significant angular-linear correlation these were used to calculate the preferred angle ( $\Phi_{max}$ ) (Batschelet, 1981). It indicates the preferred angular orientation of the polarizer (periodicity 180 deg), or the preferred azimuthal angles of the unpolarized light spots (periodicity 360 deg). The anti-preferred angle ( $\Phi_{min}$ ) was regarded as the angle perpendicular, i.e. 90 deg distant, to  $\Phi_{max}$  in the case of polarized light stimulation, and as the angle 180 deg to  $\Phi_{max}$  in the case of unpolarized light stimulation.

The angular-linear correlation analysis of stimulus–response curves gave a correlation coefficient ( $r_{al}$ ). Its square, the coefficient of determination ( $r_{al}^2$ ) ranges from zero to unity. It is an estimate of how much the change of spike rate can be explained by the change of *E*-vector/light spot angle during rotation (Bockhorst and Homberg, 2015). In order to characterize the tuning curves in more detail we calculated their amplitude and tuning width. We fitted a smoothing spline onto the stimulus–response curve of significant responses, normalized to the median BA of the respective cell, using the MATLAB curve fitting toolbox (smoothing parameter set to  $10^{-4}$ ). We defined the amplitude as the difference in normalized spike rate between peak and trough of the fit curve, and the tuning width as the angular distance between values at half-amplitude.

### Data plots

For circular histograms pooled stimulus–response curves (10 deg bin width) were plotted on a circular scale using Origin 6.0 (MicroCal, Northampton, MA, USA). Colored bars show the mean spiking activity in each bin. Error bars indicate standard deviation. For each recording, equal numbers of responses to clockwise and counterclockwise stimulation were pooled, in order to avoid a shift in tuning due to direction selectivity. Boxes in boxplots range from the 25th (Q1) to 75th (Q3) percentile. Data points less than  $Q3-1.5\times(Q3-Q1)$  and greater than  $Q3+1.5\times(Q3-Q1)$  were drawn as outliers. Whiskers extend to the adjacent value that is the most extreme data point, which is not an outlier. Notches indicate the 95% confidence interval of the median. Two medians with non-overlapping confidence intervals were termed truly different at the 5% confidence level.

## RESULTS

### General response properties

We analysed the responses of 87 CX neurons, belonging to 13 morphological types, to blue light from a dorsal direction passing a rotating polarizer, and to unpolarized green and UV light spots moving around the head of the animal. Twelve of these cell types were shown previously to be sensitive to zenithal *E*-vector orientation (Heinze et al., 2009), but one cell type (TB3) has not been studied before. Table S1 provides an overview of cell type-specific responsiveness to all three stimulation regimes. Tangential neurons of the lower division of the central body (TL neurons) receive visual input from the AOTU and represent the input stage to the polarization network of the CX (Figs 1C and 2; Heinze et al., 2009). Columnar neurons of the lower division of the central body (CL1 neurons) carry the signal to the protocerebral bridge (PB). Tangential neurons of the PB, termed TB neurons, distribute the signals throughout the 16 slices of the PB. CL1 and TB neurons represent the intermediate stage of processing (Figs 1C and 3). Columnar neurons (CPU and CP neurons) with ramifications in the PB and axonal projections to subfields of the lateral accessory lobe (LAL) probably converge on interneurons contacting descending pathways (Figs 1C and 4; Heinze and Homberg, 2009; Träger and Homberg, 2011). Therefore, these neuron types represent the output stage of visual processing of the CX.

Four types of TL neurons were studied (Fig. 2). They differ in the location of their input arborizations in the lateral accessory lobe (TL1, TL4), the medial and lateral bulb (TL2, TL3), and their axonal projections to specific layers of the lower division of the central body (CBL; Müller et al., 1997). TL1 neurons were recorded twice. One neuron responded to polarized light but not to the unpolarized light spots, whereas the other cell was responsive to all three stimuli (Fig. 2A). It was slightly excited and inhibited depending on *E*-

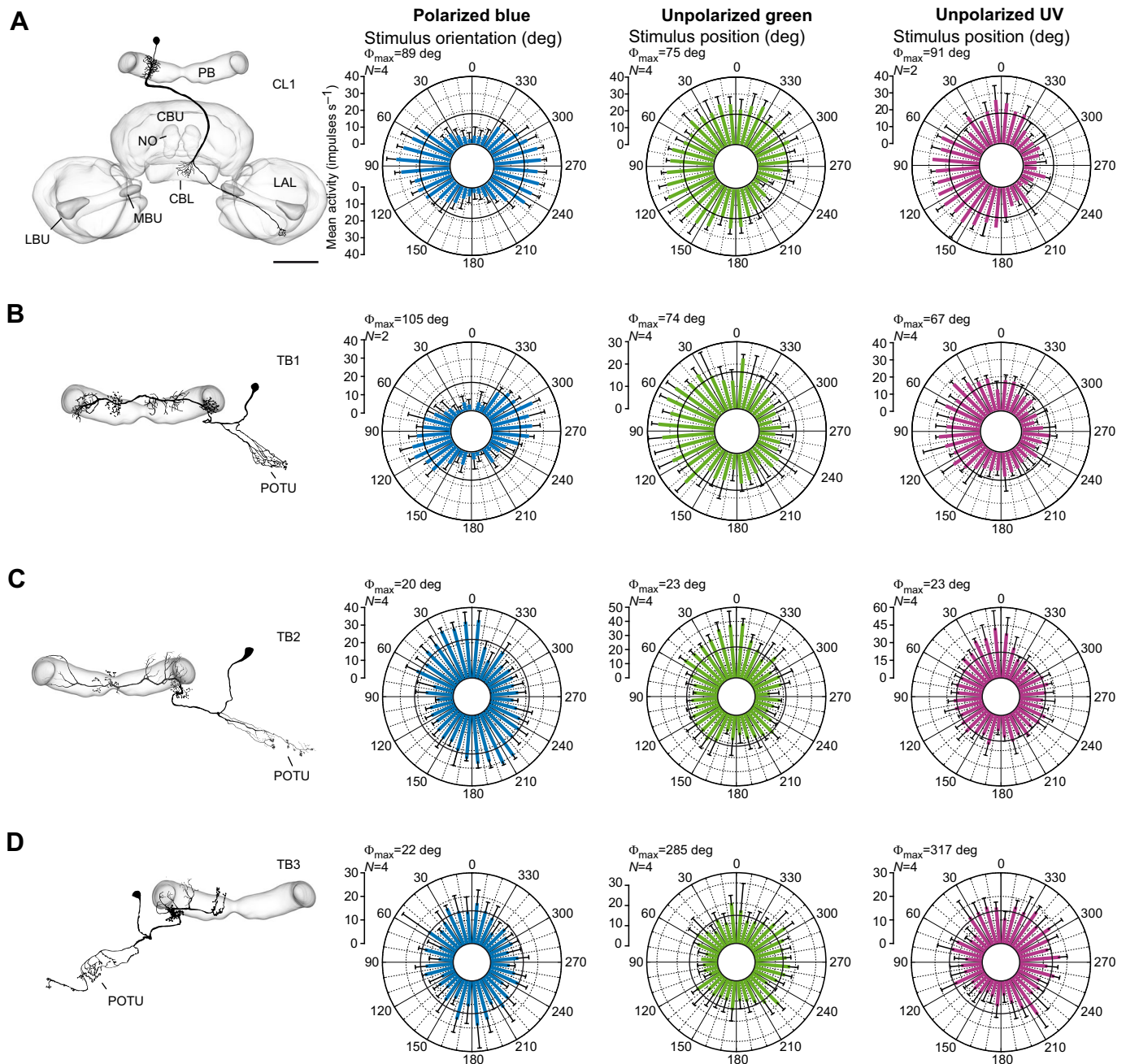


**Fig. 3. Morphology and physiology of a columnar neuron of the lower division of the central body and tangential neurons of the protocerebral bridge.** (A–D) Reconstructions of a CL1, TB1, TB2 and TB3 neuron, respectively, projected onto the standard CX (el Jundi et al., 2010; left-hand panels) and circular histograms of stimulus responses (right-hand panels).  $N$  responses to 360 deg rotations of the polarizer (polarized, blue), a green and a UV light spot (unpolarized green, unpolarized UV) were pooled and plotted as means in 10 deg bins. Black circles indicate median background activity. Error bars indicate s.d. The preferred  $E$ -vector orientation or azimuth of the unpolarized light spots is indicated by  $\Phi_{\max}$ . Scale bar, 100  $\mu\text{m}$ . CBL, central body lower division; CBU, central body upper division; PB, protocerebral bridge; CL1, columnar neuron of CBL; TB, tangential neuron of PB; LAL, lateral accessory lobe; LBU, lateral bulb; MBU, medial bulb; NO, noduli; POTU, posterior optic tubercle.

vector orientation, but excited at all angles of the green and UV light spots. The second neuron did not respond to the unpolarized light spots, but did respond to the orientation of the  $E$ -vector with excitation at all angles. TL2 neurons were recorded more frequently ( $N=7$ ). They were excited and inhibited by the  $E$ -vector (Fig. 2B; Fig. 5A). The tunings to green and UV light showed pronounced spatial opponency, i.e. excitation at the preferred angle of the unpolarized light spot and inhibition when the stimulus appeared at the opposite side of the head (anti-preferred angle; Fig. 2B;

Fig. 5A). A spike train of the TL2 neuron from Fig. 2B is shown in Fig. 1D. TL3 neurons were recorded twice. They showed polarization opponency, i.e. excitation at the preferred  $E$ -vector orientation and inhibition at the orthogonal  $E$ -vector (anti-preferred orientation; Fig. 2C; Fig. 5A). In contrast, their tunings to green and UV light were only slightly modulated by the angle of the unpolarized light spots with weak excitation at a broad range around  $\Phi_{\max}$  (Fig. 2C; Fig. 5A). Only one TL4 neuron was recorded. It showed weak excitation at  $\Phi_{\max}$ , but no inhibition at  $\Phi_{\min}$  in

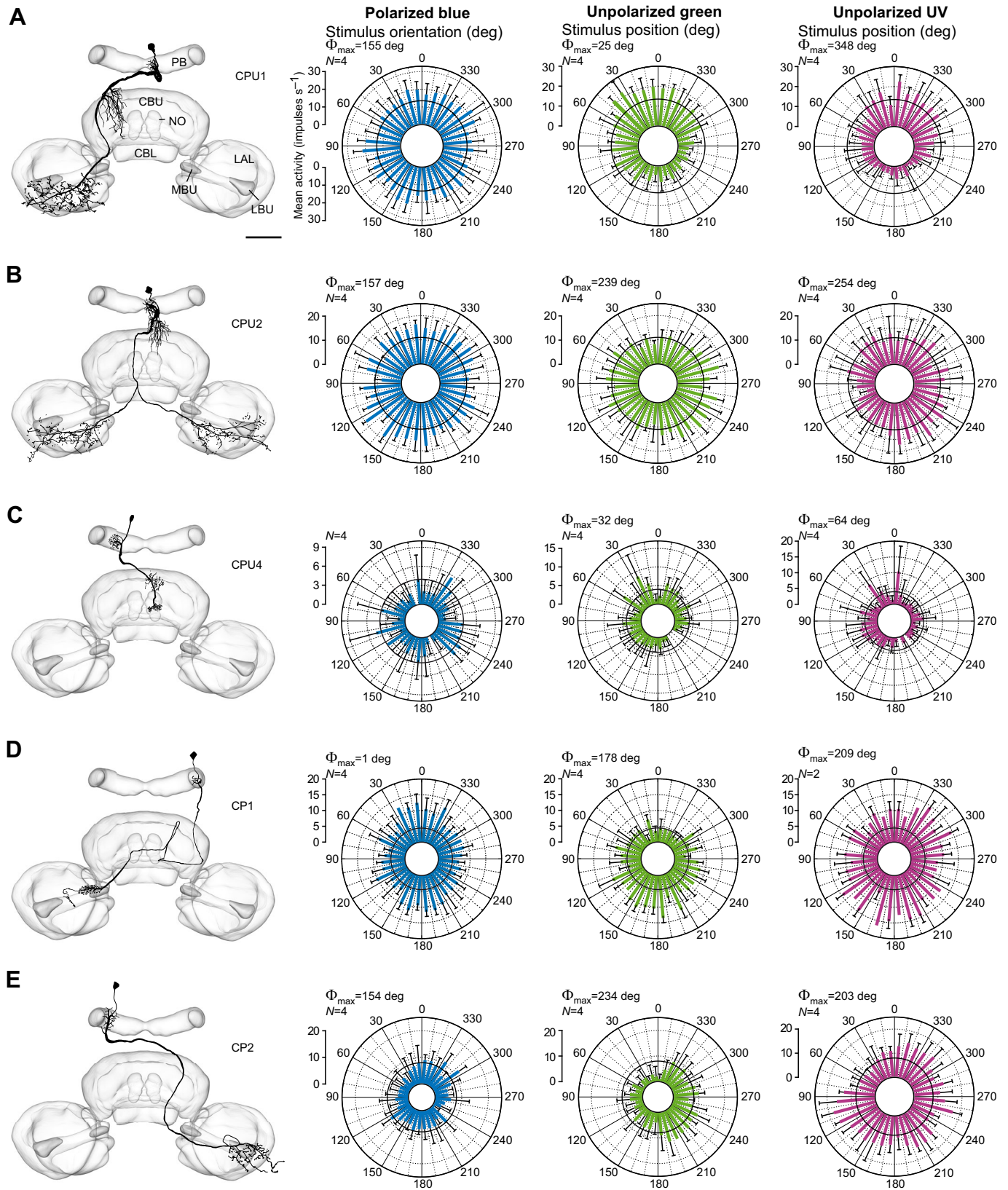


**Fig. 4. Morphology and physiology of columnar neurons (types CPU and CP) of the protocerebral bridge.** (A–E) Reconstructions of a CPU1, CPU2, CPU4, CP1 and CP2 neuron, respectively, projected onto the standard CX (el Jundi et al., 2010; left-hand panels) and circular histograms of neuronal responses (right-hand panels).  $N$  responses to 360 deg rotations of the polarizer (polarized, blue), a green and a UV light spot (unpolarized green, unpolarized UV) were pooled and plotted as means in 10 deg bins. Black circles indicate median background activity. Error bars indicate s.d. The preferred  $E$ -vector orientation or azimuth of the unpolarized light spots is indicated by  $\Phi_{\max}$ . Note that the CPU4 neuron and the CP2 neuron were not responsive to the orientation of the polarizer. Scale bar, 100  $\mu\text{m}$ . CBL, central body lower division; CBU, central body upper division; LAL, lateral accessory lobe; LBU, lateral bulb; MBU, medial bulb; NO, noduli; PB, protocerebral bridge.



response to polarized light, a strong inhibition at the anti-preferred angle of green light, and spatial opponency in response to UV light (Fig. 2D).

Four types of neuron, CL1, TB1, TB2 and TB3 of the intermediate processing stage were studied (Fig. 3). CL1 neurons connect individual slices of the CBL to slices of the PB. All CL1 neurons studied here had a mixture of fine and varicose arborizations in the CBL and claw-like varicose ramifications in the PB, characteristic of the CL1a subtype (Fig. 3A; Heinze and Homberg, 2008). The appearance of arborizations may indicate the polarity of a neuron. As shown by ultrastructural studies, smooth or fine processes are largely postsynaptic, whereas varicose or claw-like neurites generally contain transmitter-filled vesicles and act presynaptically (Peters et al., 1986; Cardona et al., 2010; Homberg and Müller, 2016). Therefore, CL1a neurons are probably pre- and postsynaptic in the CBL, and exclusively presynaptic in the PB. TB1 neurons had varicose arborizations in the posterior optic tubercle (POTU), varicose ramifications in two slices of the PB, separated by seven slices, and fine processes in several slices in between (Fig. 3B). One TB2 neuron recorded here had varicose arborizations in the outermost slice of the ipsilateral hemisphere and the innermost slices of both hemispheres of the PB and smooth processes in other slices in between. Fine processes clustered together extended to the POTU (Fig. 3C). The TB3 neuron is a novel cell type of the CX network. It had varicose ramifications in the POTU and its vicinity (Fig. 3D). In the PB it invaded the outermost and the two innermost slices of the ipsilateral hemisphere with varicose processes. Slices in between were invaded by fine processes. All neurons showed clear responses to the stimuli, but tuning characteristics were diverse. CL1 ( $N=20$ ) and TB1 ( $N=16$ ) neurons were recorded most frequently. Both cell types showed polarization and spatial opponency, but excitation and inhibition were more pronounced in the CL1 neurons (Fig. 3A,B; Fig. 5A). TB2 and TB3 neurons were recorded only once. The TB2 neuron was excited at  $\Phi_{\max}$  and inhibited at  $\Phi_{\min}$  in response to all three stimuli (Fig. 3C). Responses of the TB3 neuron were weak (Fig. 3D). The rotating polarizer elicited only slight excitation at  $\Phi_{\max}$  and slight inhibition at  $\Phi_{\min}$ . In response to the rotating light spots the neuron was clearly excited at  $\Phi_{\max}$ , and likewise inhibited at  $\Phi_{\min}$ .

Finally, four types of columnar output neurons, CPU1, CPU2, CP1 and CP2 were investigated (Fig. 4). A fifth type of neuron, CPU4, was included in this group (Fig. 4C) because like the other cell types it had dendritic ramifications in the PB, but whether it acts as an output or an intrinsic element of the CX, remains to be shown. CPU1 and CPU2 neurons had smooth ramifications in the PB and varicose ramifications in the contralateral LAL (CPU1), or both LALs (CPU2). The CPU4 neuron had varicose ramifications in the upper division of the contralateral nodulus, and in several slices of the upper division of the central body (CBU). Ramifications in the PB were smooth, thus possibly dendritic. CP1 and CP2 neurons had likewise fine, thus likely dendritic processes in the PB, and varicose terminals in distinct parts of the LAL. CPU1 ( $N=19$ ) and CPU2 ( $N=11$ ) neurons were recorded most frequently. Both cell types showed spatial opponency in their responses to the unpolarized light spots (Fig. 4A,B; Fig. 5A). CPU4 neurons were recorded only once. The neuron was not responsive to polarized light, but to both unpolarized light spots (Fig. 4C). The tunings to green and UV light were spatially opponent. CP1 neurons were recorded twice. One cell was excited at the preferred  $E$ -vector angle and at the preferred azimuth of the green spot (Fig. 4D), but both responses lacked inhibition at the anti-preferred angle. In contrast, the neuron was

excited at many angles of the UV light spot. The second neuron was not responsive to UV light, but polarization opponent in its  $E$ -vector tuning and spatially opponent in its green light tuning. CP2 neurons ( $N=4$ ) showed polarization opponency, although inhibition at  $\Phi_{\min}$  was stronger than excitation at  $\Phi_{\max}$  (Fig. 4E; Fig. 5A). Responses to the unpolarized light spots were spatially opponent, but with stronger excitation at  $\Phi_{\max}$  and weaker inhibition at  $\Phi_{\min}$  (Fig. 4E; Fig. 5A).

### Responsiveness and tuning characteristics

As shown in Figs 2–4 and illustrated in Table S1, the majority of neurons of the CX polarization processing network responded to all three stimuli. However, insensitivity to the rotating polarizer or the rotating green or UV light spots was found in neurons of all cell types and in a substantial number of tests (Table S1). Across the three stimuli some neurons of each type showed responses with significant correlation as well as responses that lacked significant correlation during the same recording. This is indicated by comparison of the total number of neurons with those that responded to each stimulus and those that did not respond to any stimulus repetition (Table S1). The overall responsiveness to polarized light, green and UV light differed between cell types. TL1 neurons showed only weak responsiveness to all three stimuli. TL2 neurons were more often responsive to the azimuth of the green spot (88%) than to the orientation of the  $E$ -vector (77%) and azimuth of the UV spot (75%) (Table S1). TL3 neurons responded more reliably to the  $E$ -vector (83%) than to the unpolarized light spots (50 and 38%). In contrast, CL1 neurons responded more reliably to green and UV light (both 73%), but less reliably to polarized light (55%), whereas TB1 neurons responded most reliably to green light (72%). CPU1 neurons showed responsiveness between 60 and 70% to all three stimuli, and finally CPU2 neurons showed lowest responsiveness (36%) to polarized light, but high responsiveness to green (68%) and UV (77%) light.

To compare the tunings to the stimuli in more detail, we plotted for each cell type all stimulus–response curves with significant correlation, normalized to the median BA of the respective neuron (Fig. 5A). Because states of background activity (BA) have a duration of up to 7 s (Bockhorst and Homberg, 2015), a minimal BA duration of 14 s was required for normalization, otherwise responses were excluded from analysis as were neurons with low sample size [TL1 ( $N=2$ ), TL4 ( $N=1$ ), TB2 ( $N=1$ ), TB3 ( $N=1$ ), CPU4 ( $N=1$ ), CP1 ( $N=2$ )].

Next we plotted tuning amplitudes and widths and the coefficient of determination ( $r_{\text{ai}}^2$ ) of the stimulus–response curves. Amplitude and width indicate the strength of modulation during stimulation by the  $E$ -vector and the unpolarized light spots. Independent of response amplitude, the correlation  $r_{\text{ai}}^2$  estimates how much the change in spike rate can be explained by the change of the stimulus angle. It therefore can be used to describe the shape of the stimulus–response curve (e.g. the more a tuning to an unpolarized light spot looks like a sinewave, the higher  $r_{\text{ai}}^2$  will be). Neurons of the input stage (TL2 and TL3) differed substantially in their tuning characteristics to polarized and unpolarized light. TL2 neurons showed higher amplitude, lower tuning width and higher correlation in azimuth tunings to the green and UV light spots. In contrast, TL3 neurons responded with higher amplitude and correlation, but with the same tuning width as TL2 neurons to the rotating polarizer (Fig. 5B–D). In all cell types downstream of TL neurons the response amplitude decreased from CL1 to CPU2 neurons (in tunings to the UV spot to similar levels in CPU1 and CPU2 neurons; Fig. 5B). The overall tuning width was similar in  $E$ -vector responses

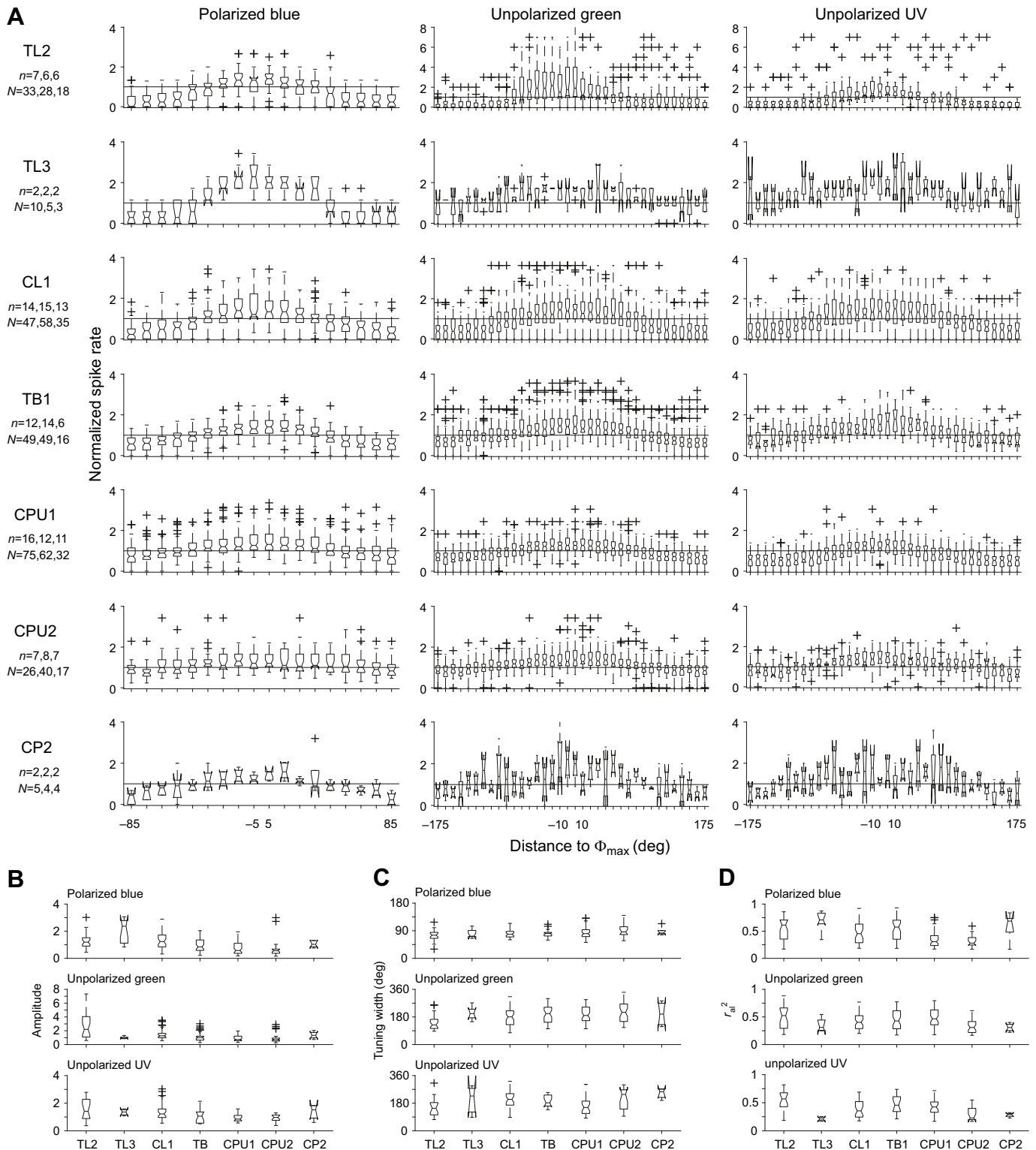


**Fig. 5. Tuning curves and tuning characteristics of responses to the plane of polarized blue light and the azimuth of an unpolarized green and UV light spot.** (A) Normalized stimulus–response curves of  $N$  responses in  $n$  neurons to polarized blue light, unpolarized green and unpolarized UV light. Stimulus–response curves were normalized to the median neuronal background activity (horizontal line at value 1).  $E$ -vector tuning was analysed from  $\Phi_{\max}-90$  deg to  $\Phi_{\max}+90$  deg, and unpolarized light spot tunings from  $\Phi_{\max}-180$  deg to  $\Phi_{\max}+180$  deg. (B–D) Box plots showing amplitude, width and  $r^2_a$  of responses in A for each cell type.

of all cell types, as indicated by the overlapping notches of boxplots (Fig. 5C). The tuning width of responses to unpolarized light was generally larger and more variable in TL3, CL1, TB1, CPU1, CPU2

and CP2 than in TL2 neurons. The correlation between  $E$ -vector angle and firing rate was generally weaker in neurons of the output stage than in input stage neurons, except in CP2 neurons (Fig. 5D).



CP2 neurons showed for all of the three stimuli a correlation similar to that of TL3 neurons (Fig. 5D).

### Polarization opponency and spatial opponency

The BA of a neuron can be highly variable during the recording despite constant recording quality (Bockhorst and Homberg, 2015). Whether a postsynaptic neuron can distinguish between states of BA or a stimulus response might depend on variability of BA. Therefore, we wanted to assess whether neurons were excited at  $\Phi_{\max}$  and inhibited at  $\Phi_{\min}$  (i.e. polarization/spatial opponency) beyond the occurring variations in BA. We calculated effective tuning amplitudes by normalizing firing rates at  $\Phi_{\max}$  ( $\pm 10$  deg) to very high (97.5th percentile) BA, and at  $\Phi_{\min}$  ( $\pm 10$  deg) to very low (2.5th percentile) BA (Fig. S1). The results are summarized in Table 1. In response to polarized light, TL3, TB1, CPU1 and CP2 neurons were excited at  $\Phi_{\max}$  and inhibited at  $\Phi_{\min}$  (Table 1, Fig. S1). Of these, TB1 and CP2 neurons showed the strongest polarization opponency. In contrast, TL2 and CL1 neurons were inhibited at  $\Phi_{\min}$ , but not excited at  $\Phi_{\max}$ . CPU2 neurons were neither excited at  $\Phi_{\max}$  above high BA nor inhibited at  $\Phi_{\min}$  below low BA. In response to the rotating green light spot, TL2, TB1 and CP2 neurons were excited at  $\Phi_{\max}$  and inhibited at  $\Phi_{\min}$ , thus showing spatial opponency (Table 1, Fig. S1). CL1 and CPU1 neurons showed no excitation at  $\Phi_{\max}$ , but inhibition at  $\Phi_{\min}$ , whereas TL3 neurons were excited but lacked inhibition. CPU2 neurons were again neither excited at  $\Phi_{\max}$  nor inhibited at  $\Phi_{\min}$ . Responses to the rotating UV light spot of TL2, TL3, TB1, CPU1 and CP2 neurons were spatially opponent (Table 1, Fig. S1). As for polarized and green light stimulation, CL1 neurons showed no excitation at the preferred angle and CPU2 neurons no inhibition at the anti-preferred angle.

**Table 1. Polarization/spatial opponency in CX neurons of *Schistocerca gregaria***

Cell type	Excitation at $\Phi_{\max}$	Inhibition at $\Phi_{\min}$
Polarized blue		
TL2	0	–
TL3	++	–
CL1	0	–
TB1	++	–
CPU1	+	–
CPU2	0	0
CP2	++	–
Unpolarized green		
TL2	+	–
TL3	+	0
CL1	0	–
TB1	+	–
CPU1	0	–
CPU2	0	0
CP2	++	–
Unpolarized UV		
TL2	+	–
TL3	+	–
CL1	0	–
TB1	+	–
CPU1	+	–
CPU2	+	0
CP2	+	–

Effective excitation at  $\Phi_{\max}$  and effective inhibition at  $\Phi_{\min}$  for responses with significant correlation to polarized blue, unpolarized green and unpolarized UV stimulation. Robust excitation (inhibition) is denoted by ++ (–), and partial excitation (inhibition) by + (–). '0' denotes no effective excitation/inhibition.

### Dependency on background activity

Background firing may be highly variable between different recordings of the same neuron type (Heinze and Homberg, 2009), and it has already been suggested that in CPU neurons low BA might indicate strong responses to polarized light (Bockhorst and Homberg, 2015). To compare responses that occurred during high BA to responses that occurred during low BA, we sorted recordings of each cell type according to their median BA into those with high BA and those with low BA (for detailed description, see Materials and methods). The calculated cell-type specific BA of TL2, CL1, TB1, CPU1 and CPU2 neurons was 9, 8, 20, 17 and 11 spikes  $s^{-1}$ , respectively. Across all stimulation regimes and cell types the tuning shape was dependent on BA (Fig. 6A; Fig. S2A, S3A). In TL2, CL1, TB1 and CPU1 neurons the amplitude of responses to the rotating green light spot and its variability were significantly higher during low BA than during high BA (Fig. 6B). In CPU2 neurons only the variability of amplitude was increased in neurons with low BA. In contrast, the range of tuning width was generally independent of BA, but the median width was shifted towards 180 deg in TB1, CPU1 and CPU2 neurons (Fig. 6C). The distribution of  $r_{\text{al}}^2$  in neurons with high BA was similar to the distribution of  $r_{\text{al}}^2$  in neurons with low BA in CL1, TB1, CPU1 and CPU2 neurons, but significantly decreased in TL2 neurons with low BA (Fig. 6D). CPU2 neurons showed lowest  $r_{\text{al}}^2$  independent of BA. Tunings to the rotating UV light spot showed similar properties (Fig. S2). The amplitude was higher in TB1, CPU1 and CPU2 neurons with low BA than in cells with high BA (Fig. S2B). Again the width of tuning was statistically equal in all cell types during high and low BA, but the median shifted towards 180 deg in TL2, TB1, CPU1 and CPU2 neurons during low BA (Fig. S2C). The  $r_{\text{al}}^2$  of UV tunings was independent of BA in all cell types (Fig. S2D). In responses of TB1, CPU1 and CPU2 neurons to the rotating polarizer the amplitude was higher in cells with low BA than in cells with high BA (Fig. S3A,B). Amplitude variability was increased in all cell types. As in the other stimulation regimes, tuning widths were equal during high BA and low BA across all cell types (Fig. S2C). The correlation between *E*-vector orientation and firing rate was higher in CPU2 neurons during low BA than during high BA, and not affected by BA in all other cell types (Fig. S2D).

We next investigated whether polarization opponency and spatial opponency also depended on BA. Thus we plotted again the firing rates at  $\Phi_{\max}$  and  $\Phi_{\min}$  normalized to very high and very low levels of BA, respectively, in the two populations of neurons (Fig. S4). The main findings are shown in Table 2. In response to polarized light during high BA, only TL2 and TB1 neurons showed polarization opponency (Table 2). In contrast, CL1 and CPU2 neurons were inhibited at  $\Phi_{\min}$ , but not excited at  $\Phi_{\max}$ , respectively. CPU1 neurons were neither excited at  $\Phi_{\max}$  above high BA nor inhibited at  $\Phi_{\min}$  below low BA. In contrast, during low BA all cell types except CPU2 neurons showed polarization opponency. Only TL2 neurons showed spatial opponency in green light spot responses at high BA. All other cell types lacked excitation at  $\Phi_{\max}$ . In contrast, during low BA TL2, TB1 and CPU1 neurons were spatially opponent. CL1 neurons were again inhibited at  $\Phi_{\min}$ , but not excited at  $\Phi_{\max}$ , and CPU2 neurons were neither excited at  $\Phi_{\max}$  above high BA nor inhibited at  $\Phi_{\min}$  below low BA. Responses to the rotating UV light spot during high BA showed spatial opponency in TL2 and CPU1 neurons. Again, CL1 neurons were inhibited at  $\Phi_{\min}$ , but not excited at  $\Phi_{\max}$ . In contrast, during low BA all cell types except CL1 neurons responded in a spatially opponent manner. In general, cells were mainly inhibited when they had high BA. In contrast, they were strongly excited during low BA, but the

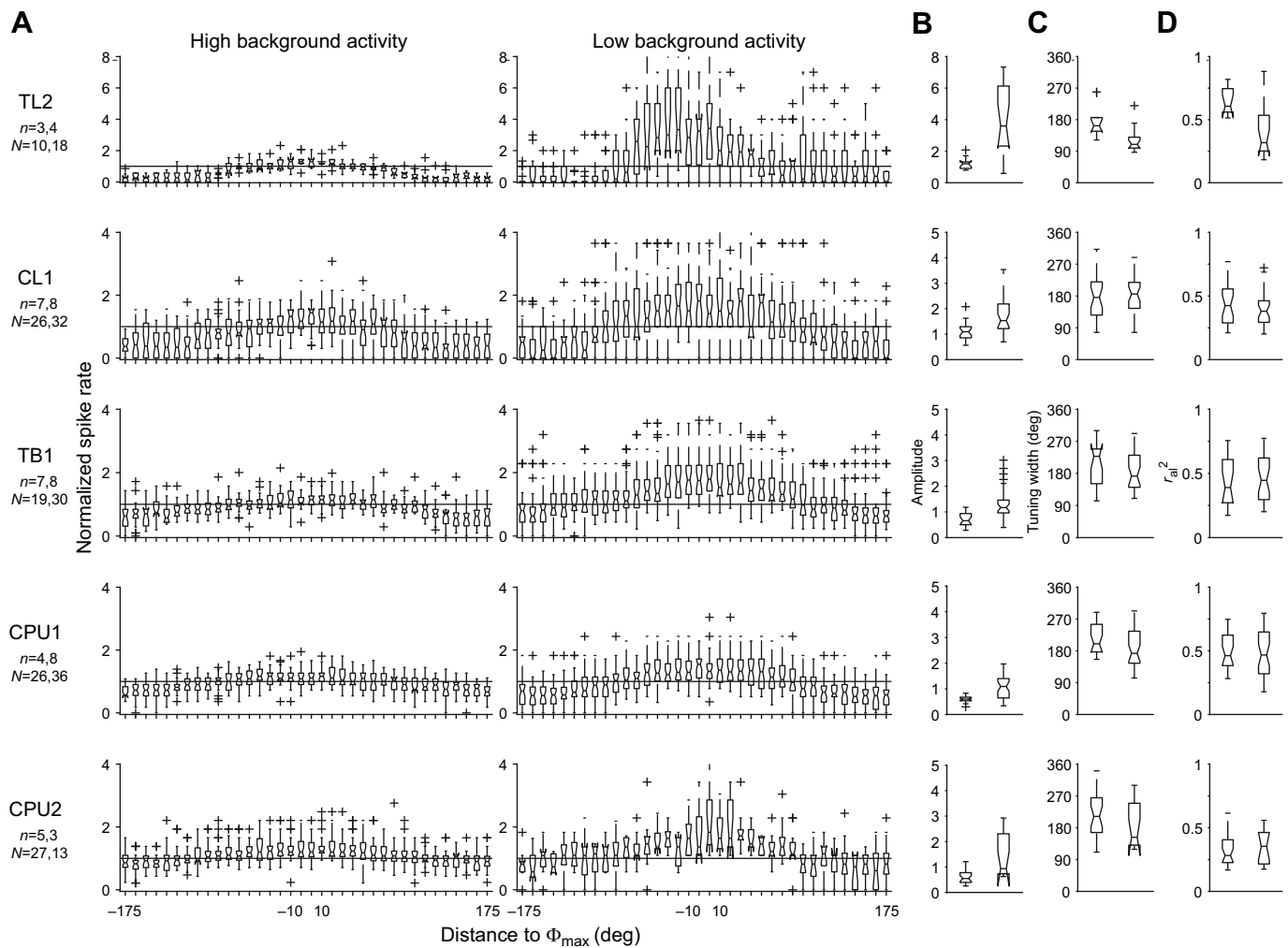


**Fig. 6. Comparison of tuning characteristics to green light during high and low background activity.** (A) Normalized stimulus–response curves of  $N$  responses in  $n$  neurons to unpolarized green light during high and low neuronal background activity. Stimulus–response curves were normalized to the median neuronal background activity (horizontal line at value 1).  $E$ -vector tunings were analysed from  $\Phi_{max}-90$  deg to  $\Phi_{max}+90$  deg, and green/UV light spot tunings from  $\Phi_{max}-180$  deg to  $\Phi_{max}+180$  deg. (B–D) Box plots showing amplitude, width and  $r_{ai}^2$  of responses in A for each cell type during high (left) and low (right) BA.

inhibition at  $\Phi_{min}$  remained, although weaker than during high BA, so that polarization and spatial opponency was more distinct.

### Rotation direction sensitivity

For the calculation of general response characteristics of a neuron, such as the preferred tuning angle, rotation-direction specific effects were eliminated by pooling equal numbers of clockwise and counterclockwise rotations. Here, we address possible differences in response parameters depending on the direction of rotation. We calculated for each neuron the angular distances between  $\Phi_{max}$  values of individual responses to clockwise and counterclockwise rotations to the pooled  $\Phi_{max}$  of responses to all rotations. Neurons usually showed either delayed responses during single rotations (Fig. S5) or advanced responses (Fig. 7) in comparison with the pooled  $\Phi_{max}$  from equal numbers of clockwise and counterclockwise rotations. Neurons showing a mixture of advanced and delayed responses were excluded from the analysis. In anticipatory  $E$ -vector tunings of all cell types, time shifts were rather similar, except in CP2 neurons (Fig. 7). In contrast, responses to the green light spot showed increasingly longer time shifts from the input towards the output processing stage. Especially in CPU2 neurons time shifts were more negative than in all other cell types.

Also the overall time shifts of all cell types were usually twice as long in green and UV responses than in  $E$ -vector tunings. In neurons showing a delayed  $\Phi_{max}$  in single rotations compared with the pooled  $\Phi_{max}$ s, the delays were generally shorter in  $E$ -vector and green light tunings than the advances of anticipating cells (Fig. S5; Fig. 7). In UV light spot tunings time delays were similar in absolute value to time advances of anticipating cells. The overall occurrence of advances and delays was similar in CL and TB neurons, but in TL2 and all neurons of the output stage, phase advances in  $\Phi_{max}$  dominated.

### Angular distance between tunings to different stimuli

Although the solar position changes over the course of the day, there is a fixed relationship between sun position and sky polarization (Fig. 1). Important for navigational purposes, the  $E$ -vector in the zenith is always 90 deg distant (orthogonal) from the solar azimuth (Fig. 1A). To assess whether this is reflected in the tuning of CX neurons, we calculated the angular distance between the azimuth of green tuning and the azimuth of UV tuning, and between the orientation of polarization tuning and the azimuth of green/UV tuning. Distances between  $\Phi_{max}$  green and  $\Phi_{max}$  UV were clustered around 0 deg in CL1, TB, CPU1 and CPU2 neurons (Fig. 8A). In TL neurons the

**Table 2. Polarization and spatial opponency in CX neurons with low and high BA**

Cell type	Responses from neurons with high BA		Responses from neurons with low BA	
	Excitation at $\Phi_{\max}$	Inhibition at $\Phi_{\min}$	Excitation at $\Phi_{\max}$	Inhibition at $\Phi_{\min}$
Polarized blue				
TL2	+	–	+	–
CL1	0	–	+	–
TB1	++	–	++	–
CPU1	0	0	++	–
CPU2	0	–	++	0
Unpolarized green				
TL2	+	–	++	–
CL1	0	–	0	–
TB1	0	–	++	–
CPU1	0	–	+	–
CPU2	0	0	0	0
Unpolarized UV				
TL2	+	–	+	–
CL1	0	–	0	–
TB1	0	–	++	–
CPU1	+	–	+	–
CPU2	+	0	++	–

Effective excitation at  $\Phi_{\max}$  and effective inhibition at  $\Phi_{\min}$  for responses with significant correlation to polarized blue, unpolarized green and unpolarized UV stimulation. Responses were divided into those from neurons with high BA and those from neurons with low BA. Robust excitation (inhibition) is denoted by ++ (–), and partial excitation (inhibition) by + (–). '0' denotes no effective excitation/inhibition.

dispersion was higher, so that the Rayleigh test did not reveal any clustering. In certain cell types (CL1, CPU1) single distances were close to 180 deg. Comparison of *E*-vector and light-spot tuning showed that most TL neurons had a tuning distance close to 90 deg (Fig. 8B). However, most of the TL neurons clustered around 90 deg belonged to the TL2 or TL3 subtypes, whereas the TL1 and TL4 neurons showed different tuning distances of 17 deg (TL1) and 153 deg (TL4). In contrast, angular distances in CL1 neurons between *E*-vector and unpolarized light spot tuning ranged from 0 to 180 deg. In TB neurons the distribution of distances was non-directional when comparing *E*-vector tuning with green tuning, but directed toward 0 deg when comparing *E*-vector tuning with UV tuning. CPU2 and CP neurons showed non-directional distribution of angular distances. In CPU1 neurons distances were clustered around 70 deg, but only for comparison of *E*-vector tuning with green tuning. CPU2 and CP1/CP2 neurons showed no clustering of angular distances.

## DISCUSSION

### Contribution of chromatic cues to the internal *E*-vector compass

We analysed the responses of locust CX neurons to zenithal *E*-vectors and to unpolarized green and UV light spots moving on a circular path around the head of the animal. All types of CX neurons that were sensitive to zenithal *E*-vector orientation were also sensitive to the azimuth of the unpolarized light spots. Therefore, CX neurons are well suited to code for solar azimuth. Similar responses of CX neurons to a moving bright object have been demonstrated in flies (Seelig and Jayaraman, 2015; Kim et al., 2017), cockroaches (Varga and Ritzmann, 2016), monarch butterflies (Heinze and Reppert, 2011) and two species of dung beetle (el Jundi et al., 2015). In the locust, tuning to unpolarized UV light was similar to tuning to green light across all cell types. Neurons of the AOTU, located upstream of CX neurons, showed

color opponent tuning to green and UV light (Pfeiffer and Homberg, 2007). Commissural neurons connecting the right and left AOTUs (types LoTu1 and TuTu1) were inhibited by UV light and excited by green light at the same azimuth and vice versa (Pfeiffer and Homberg, 2007). These neurons were thus assumed to encode for the chromatic differences in the solar and antisolar hemisphere of the sky. In all types of CX neurons, however, tuning to the green and UV light spots were highly similar. We therefore assume that these neurons, in addition to celestial *E*-vector orientation, code for the azimuth of bright light sources, possibly representing the sun, largely ignoring wavelength information. This is consistent with wavelength independent azimuth coding in the CX of the monarch butterfly (Heinze and Reppert, 2011), and in a small subset of locust CX neurons (el Jundi et al., 2014a).

The tuning of TL2 and TL3 neurons showed a 90 deg distance between the  $\Phi_{\max}$  of the zenithal *E*-vector and  $\Phi_{\max}$  of the green light spot, reflecting the relationship between solar azimuth and zenithal *E*-vector in the sky (Fig. 1A). In all cell types downstream in the network this relationship occurred only in a minority of recorded cells. TL neurons integrate *E*-vector orientations across the entire sky in a matched filter-like manner for particular solar positions (Bech et al., 2014). Therefore, the 90 deg relationship of solar azimuth and zenithal *E*-vector orientation strongly supports the animal's internal polarization compass at the input stage of the CX. Neurons of the AOTU were reported to show a daytime compensation in the angular distance between *E*-vector and light spot tuning (Pfeiffer and Homberg, 2007). In contrast, tuning distances may be daytime independent in TL2 and TL3 neurons. TL1 and TL4 neurons showed striking deviations from a 90 deg tuning relation with tuning distances close to 0 and 180 deg, but their receptive field organizations are not known. For all other CX neurons of the polarization network, receptive fields for *E*-vector orientations have likewise not been analysed in detail, so that it is still unknown whether the 'matched filter' properties of TL neurons are maintained in all neurons downstream in the network. Because of the mean distance between polarization and azimuth tuning of 70 deg, receptive fields of CPU1 neurons are likely to differ from those of TL neurons. In the monarch butterfly angular distances between the preferred *E*-vector and the preferred azimuth of a green spot were less than 45 deg in TL neurons (Heinze and Reppert, 2011), while in dung beetles they ranged from 0 to 90 deg across all recorded cell types (TL, CL1, TB1 and CPU1) (el Jundi et al., 2015). In neither species have the receptive fields for polarized light been characterized in CX neurons yet.

### Signal processing from input to output of the CX network

At least two parallel input pathways to the CBL exist in the fruit fly (Omoto et al., 2017), the honeybee (Held et al., 2016) and the locust (Homberg et al., 2003). In *Drosophila*, two types of AOTU neurons making connections to two distinct types of ring neurons (TL neurons) responded differently to a moving unpolarized light spot. Equivalent cell types in the locust may be the two subtypes of TULAL1 neurons, making synapses with TL2 neurons in the lateral bulb (TULAL1a) and with TL3 neurons in the lateral and medial bulb (TULAL1b) (Träger et al., 2008). In our experiments TL2 and TL3 showed remarkably different response amplitudes to polarized and unpolarized light, but the sample size for TL3 neurons was low, so that further experiments on TL3 neurons are necessary to substantiate this observation. In contrast to TL2 and TL3 neurons, the role of TL1 and TL4 neurons is unknown. Their dendritic arbors spread widely through the LAL and thus might receive input from a variety of neurons. Both recorded TL1 neurons were responsive to the orientation of the *E*-vector, but only



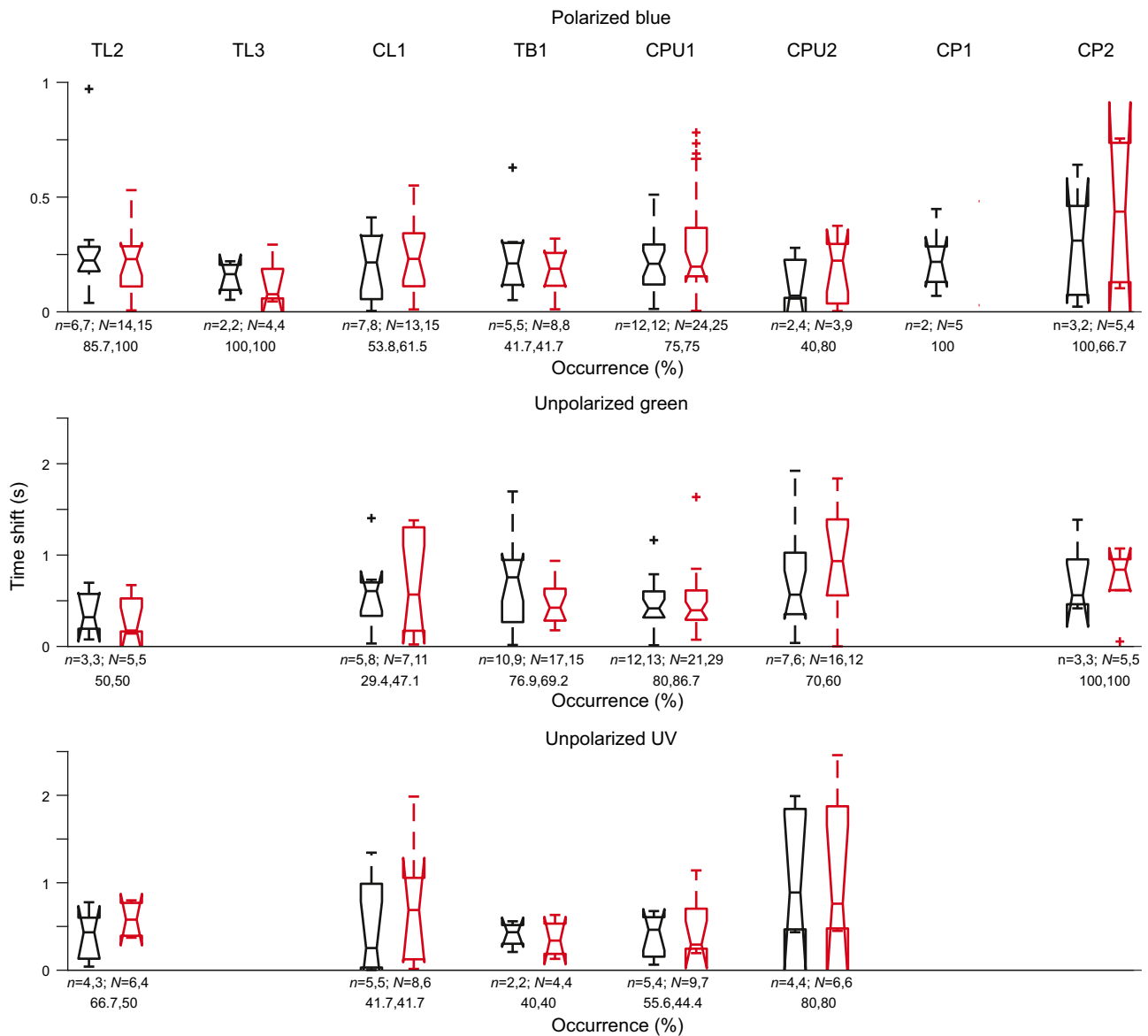


**Fig. 7. Response advances in responses to clockwise and counterclockwise stimulation.** Box plots showing phase advance shifts in  $\Phi_{\max}$  from individual responses to clockwise (black) and counterclockwise (red) rotations when compared with the pooled  $\Phi_{\max}$  of responses to all rotations.  $n$ , number of neurons;  $N$ , number of clockwise and counterclockwise rotations. Only cell types with  $N > 2$  are included. In recordings with different numbers of clockwise and counterclockwise responses, redundant responses were excluded from analysis randomly.

one of them was responsive to the azimuth of the unpolarized light spots. The TL4 neuron was tuned to the zenithal  $E$ -vector and to the azimuth of the unpolarized green and UV light spots. Hence all subtypes of TL neurons studied here seem to be involved in sky-compass coding, but may differ in the relative contribution and combination of different celestial signals.

In all cell types downstream of TL neurons the responses to the polarized and the unpolarized light stimuli were generally similar, indicating that polarization and azimuth information are processed together. Bockhorst and Homberg (2015) reported high variability in  $E$ -vector tuning at the output processing stage (CPU2 neurons) ranging from strong polarization opponency to unresponsiveness. In the present study, CPU2 neurons showed overall lowest responsiveness to  $E$ -vector orientation. Moreover, their tunings to all three stimuli were generally of low amplitude and showed weak correlation with little variability. A high incidence of unresponsiveness of CPU2 neurons to zenithal  $E$ -vectors (50%) was also observed by Heinze and Homberg (2009).

They suggested that CPU2 neurons are recruited to the polarization processing network depending on the animal's internal state (Heinze and Homberg, 2009). It is thus conceivable that in CPU2 neurons context information plays a major role, so that the moving visual scenery as presented to the animal by Bockhorst and Homberg (2015) may have resulted in a higher incidence of pronounced responses.

CX neurons usually show some variability in background spiking over the course of a recording (Bockhorst and Homberg, 2015). We thus analysed spiking at  $\Phi_{\max}$  and  $\Phi_{\min}$  to different levels of background activity (BA). Polarization and spatial opponency occurred in all cell types except CL1 and CPU2 neurons. The exclusive inhibition of CL1 neurons by polarized light and the resultant lack of polarization opponency have already been shown (Bockhorst and Homberg, 2015). It is therefore likely that polarization and spatial opponency in the PB emerge from mutual inhibition of TB1 neurons with opposite  $E$ -vector (Bockhorst and Homberg, 2015) and green/UV light spot tuning. Polarization

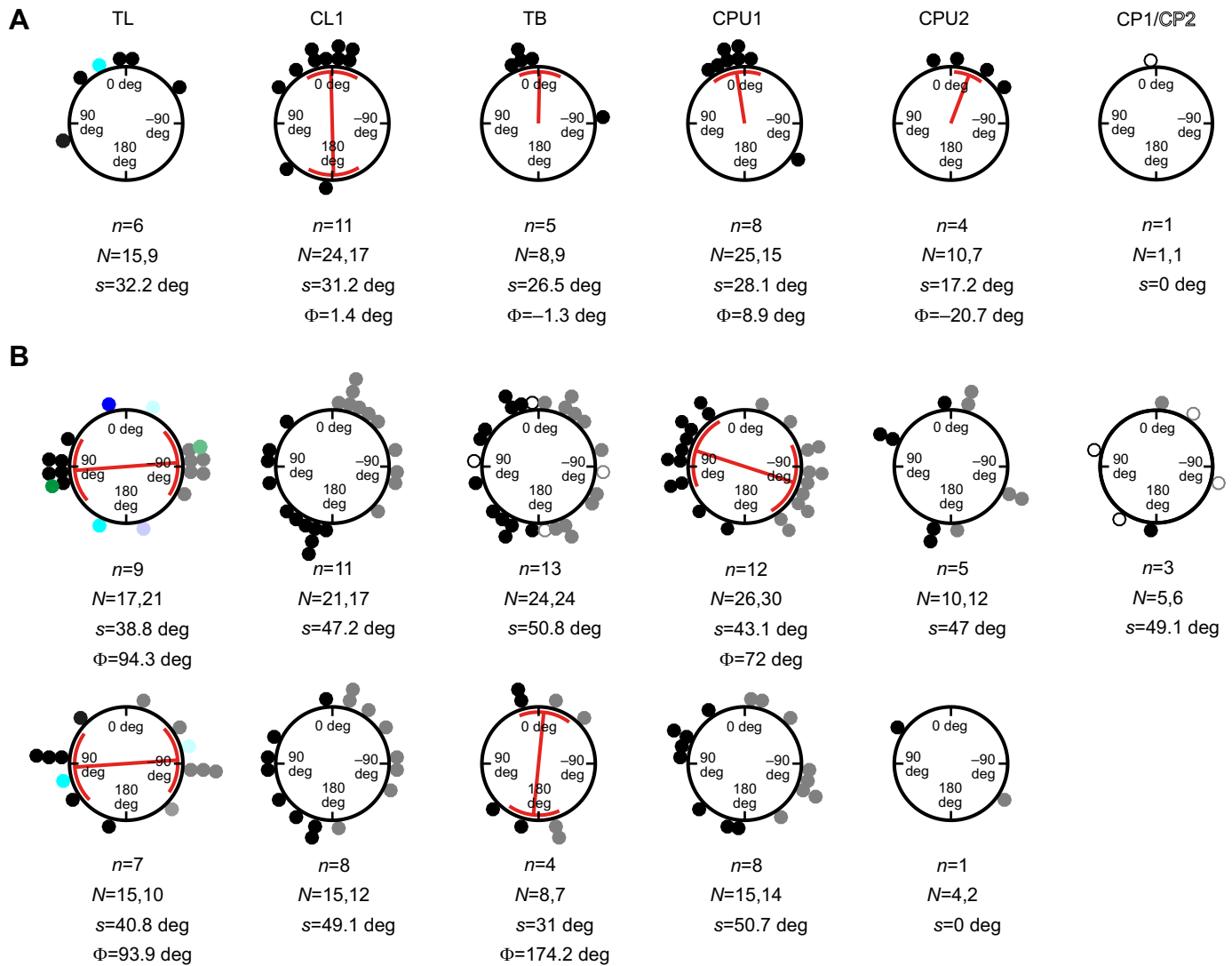


**Fig. 8. Distance between tunings to polarized light, unpolarized green and UV light spots.** (A) Relative distances between  $\Phi_{\max}$  green and  $\Phi_{\max}$  UV from  $n$  neurons. Pooled  $\Phi_{\max}$  were calculated from  $N$  responses to clockwise stimulation and  $N$  responses to counterclockwise stimulation (green, UV). (B) Positive relative angular distances (filled black and colored circles) and negative angular distances (filled gray and light-colored circles) between the  $\Phi_{\max}$  of  $E$ -vector tuning and the  $\Phi_{\max}$  of unpolarized green tuning (upper panel) and between the  $\Phi_{\max}$   $E$ -vector tuning and the  $\Phi_{\max}$  of unpolarized UV tuning (lower panel) from  $n$  neurons. Pooled  $\Phi_{\max}$  values were calculated from  $N$  responses to clockwise stimulation and  $N$  responses to counterclockwise stimulation (polarized blue, unpolarized green/polarized blue, unpolarized UV). Values of CP2, TB2 and TB3 neurons are plotted in open circles, those of TL1 in blue, TL2 in black, TL3 in green, and TL4 neurons in cyan circles. The distribution of angular distances was statistically tested for uniformity using the Rayleigh test (Batschelet, 1981). In panel B angles were doubled in all cases and in panel A whenever the distribution appeared bidirectional. In the case of significance ( $P < 0.05$ ) the direction of the mean vector ( $\Phi$ ) is given and plotted (red line). 's' denotes circular standard deviation (red), plotted in significant cases only.

opponency was reported by Bockhorst and Homberg (2015) to be absent in CX neurons upstream of TB1 neurons, but they considered only CL1 and TL2 neurons. Here we show that  $E$ -vector tunings of another type of TL neuron (TL3) are polarization opponency. In contrast to TL3 neurons, TL2 neurons were exclusively inhibited by polarized light, but spatially opponent in their responses to green light. This raises the question of how polarization opponency in TL2 neurons and spatial opponency in TL3 neurons leads to exclusive inhibition of CL1 neurons under rigorous criteria. CL1 neurons probably receive input from six morphological types of TL neuron. At least four of them (TL1–4) are probably involved in shaping  $E$ -vector and azimuth tuning of CL1 neurons. TL2, TL3 and TL4 neurons are GABA immunoreactive (Homberg et al., 1999) and therefore probably inhibit CL1 neurons. Although the TL2 neurons shown here were strongly inhibited by all stimuli at  $\Phi_{\min}$ , the total

excitation of TL3 and possibly TL4 neurons might be dominant, resulting in an overall inhibition of the postsynaptic CL1 neurons.

### Parallels to the mammalian brain

We compared responses of neurons with high and low BA. In all cell types low BA was accompanied by enhanced response amplitudes to all stimuli, as well as enhanced variability in response amplitude. Likewise, neuronal BA influences behavioral performance in human vision (Boly et al., 2007) and somatosensation (Hesselmann et al., 2008). Two models explaining the interaction of BA and stimulus-evoked activity are under discussion. BA may be superimposed on the evoked neuronal response as shown in the cat V1 cortex (Arieli et al., 1969; Azouz and Gray, 1999) and in human extrastriate areas (Becker et al., 2011). In contrast, a recent study indicates that ongoing activity in human cerebral cortex negatively correlates with evoked activity,

such that evoked responses are of higher amplitude whenever pre-stimulus activity is low (He, 2013). Neurons of the locust CX polarization vision network seem to share the latter characteristics, suggesting that they integrate different stimuli in a non-linear way. As in the cat and human cortex this interaction between background and evoked firing might be interpreted as some kind of attention related to the internal neuronal state. In most neurons polarization and spatial opponency were enhanced at low BA. This suggests that background firing in the locust CX strongly interacts with navigational task-evoked responses.

All recorded cell types showed a shift in  $\Phi_{\max}$  of unpolarized light spot or *E*-vector tuning depending on the direction of stimulus rotation (clockwise or counterclockwise), as already demonstrated for polarized light (Träger and Homberg, 2011; Bockhorst and Homberg, 2015). Cells either responded with phase advances to *E*-vector orientation and light spot azimuth, or their firing was phase delayed when comparing clockwise and counterclockwise stimulation. These phenomena appear similar to the anticipatory firing observed in rat head-direction cells of the anterodorsal thalamus (AND) and postsubiculum (PoS) (Taube and Muller, 1998). Cells of the AND anticipate future headings, but cells of the PoS are tuned to past headings. In the locust, TL, CL, TB1, CPU1 and CPU2 neurons might encode both, future headings or past headings. The two phenomena occurred equally often in CL and TB1 neurons, but in all output neurons phase advances were clearly more prominent. In rat head-direction cells, anticipation is assumed to arise from motor efference copies and vestibular input (van der Meer et al., 2007). Because the locust was fixed during the experiments, anticipation in the CX might arise solely from stimulus history or the velocity of stimulus rotation. Rotation velocity might influence anticipation, because CPU2 neurons anticipated future *E*-vector orientations by more than 500 ms with a rotation velocity of 30 deg s<sup>-1</sup> (Bockhorst and Homberg, 2015), but only about 250 ms at rotation velocities of 40 and 36 deg s<sup>-1</sup>, as used here. Stimulus anticipation was also dependent on the type of stimulus. In most cell types anticipatory time shifts of the preferred azimuth of the green/UV spot (360 deg periodicity) were twice as long as those of the preferred *E*-vector orientation (180 deg periodicity). This dependence on stimulus periodicity also points to a mechanism based on stimulus history. Nonetheless, for elucidating the origin of anticipation in locust compass cells it will be essential to study anticipation in actively and passively moving animals, and to test various stimulus velocities.

#### Acknowledgements

We thank Joss von Hadeln for providing the drawings of the TB2 and TB3 neurons and Martina Kern for maintaining locust cultures.

#### Competing interests

The authors declare no competing or financial interests.

#### Author contributions

Conceptualization: K.P., U.H.; Methodology: U.P., K.P., U.H.; Software: U.P., K.P., U.H.; Validation: U.P., U.H.; Formal analysis: U.P.; Investigation: U.P.; Resources: U.H.; Data curation: U.P.; Writing - original draft: U.P.; Writing - review & editing: U.P., K.P., U.H.; Visualization: U.P.; Supervision: K.P., U.H.; Project administration: U.H.; Funding acquisition: U.H.

#### Funding

This work was supported by the Deutsche Forschungsgemeinschaft (grant HO 950/23-1).

#### Supplementary information

Supplementary information available online at <http://jeb.biologists.org/lookup/doi/10.1242/jeb.171207.supplemental>

#### References

- Arieli, A., Sterkin, A., Grinvald, A. and Aertsen, A. (1969). Dynamics of ongoing activity: explanation of the large variability in evoked cortical responses. *Science* **273**, 1868-1871.
- Azouz, R. and Gray, C. M. (1999). Cellular mechanisms contributing to response variability of cortical neurons *in vivo*. *J. Neurosci.* **19**, 2209-2223.
- Batschelet, E. (1981). *Circular Statistics in Biology*. London, UK: Academic Press.
- Bech, M., Homberg, U. and Pfeiffer, K. (2014). Receptive fields of locust brain neurons are matched to polarization patterns of the sky. *Curr. Biol.* **24**, 2124-2129.
- Becker, R., Reinacher, M., Freyer, F., Villringer, A. and Ritter, P. (2011). How ongoing neuronal oscillations account for evoked fMRI variability. *J. Neurosci.* **31**, 11016-11027.
- Berens, P. (2009). CircStat: a MATLAB toolbox for circular statistics. *J. Stat. Softw.* **31**, 1-21.
- Bockhorst, T. and Homberg, U. (2015). Amplitude and dynamics of polarization-plane signaling in the central complex of the locust brain. *J. Neurophysiol.* **113**, 3291-3311.
- Boly, M., Baiteau, E., Schnakers, C., Degueldre, C., Moonen, G., Luxen, A., Phillips, C., Peigneux, P., Maquet, P. and Laureys, S. (2007). Baseline brain activity fluctuations predict somatosensory perception in humans. *Proc. Natl. Acad. Sci. USA* **104**, 12187-12192.
- Brines, M. L. and Gould, J. L. (1979). Bees have rules. *Science* **206**, 571-573.
- Cardona, A., Saalfeld, S., Preibisch, S., Schmid, B., Cheng, A., Pulokas, J., Tomancak, P. and Hartenstein, V. (2010). An integrated micro- and macroarchitectural analysis of the *Drosophila* brain by computer-assisted serial section electron microscopy. *PLoS Biol.* **8**, e1000502.
- Clements, A. N. and May, T. E. (1974). Studies on locust neuromuscular physiology in relation to glutamic acid. *J. Exp. Biol.* **60**, 673-705.
- Coemans, M. A. J. M., Vos Hzn, J. J. and Nuboer, J. F. W. (1994). The relation between celestial colour gradients and the position of the sun, with regard to the sun compass. *Vision. Res.* **34**, 1461-1470.
- Dacke, M., Nordström, P. and Scholtz, C. H. (2003). Twilight orientation to polarised light in the crepuscular dung beetle *Scarabaeus zambesianus*. *J. Exp. Biol.* **206**, 1535-1543.
- el Jundi, B., Heinze, S., Lenschow, C., Kurylas, A., Rohlfing, T. and Homberg, U. (2010). The locust standard brain: a 3D standard of the central complex as a platform for neural network analysis. *Front. Syst. Neurosci.* **3**, 3-21.
- el Jundi, B., Pfeiffer, K. and Homberg, U. (2011). A distinct layer of the medulla integrates sky compass signals in the brain of an insect. *PLoS ONE* **6**, e27855.
- el Jundi, B., Pfeiffer, K., Heinze, S. and Homberg, U. (2014a). Integration of polarization and chromatic cues in the insect sky compass. *J. Comp. Physiol. A* **200**, 575-589.
- el Jundi, B., Smolka, J., Baird, E., Byrne, M. J. and Dacke, M. (2014b). Diurnal dung beetles use the intensity gradient and the polarization pattern of the sky for orientation. *J. Exp. Biol.* **217**, 2422-2429.
- el Jundi, B., Warrant, E. J., Byrne, M. J., Khaldy, L., Baird, E., Smolka, J. and Dacke, M. (2015). Neural coding underlying the cue preference for celestial orientation. *Proc. Natl. Acad. Sci. USA* **112**, 11395-11400.
- Frost, B. J. and Mouritsen, H. (2006). The neural mechanisms of long distance animal navigation. *Curr. Opin. Neurobiol.* **16**, 481-488.
- Gould, J. L. (1998). Sensory bases of navigation. *Curr. Biol.* **8**, R731-R738.
- He, B. J. (2013). Spontaneous and task-evoked brain activity negatively interact. *J. Neurosci.* **33**, 4672-4682.
- Heinze, S. and Homberg, U. (2007). Maplike representation of celestial *E*-vector orientations in the brain of an insect. *Science* **315**, 995-997.
- Heinze, S. and Homberg, U. (2008). Neuroarchitecture of the central complex of the desert locust: intrinsic and columnar neurons. *J. Comp. Neurol.* **511**, 454-478.
- Heinze, S. and Homberg, U. (2009). Linking the input to the output: new sets of neurons complement the polarization vision network in the locust central complex. *J. Neurosci.* **29**, 4911-4921.
- Heinze, S. and Reppert, S. M. (2011). Sun compass integration of skylight cues in migratory monarch butterflies. *Neuron* **69**, 345-358.
- Heinze, S., Gotthardt, S. and Homberg, U. (2009). Transformation of polarized light information in the central complex of the locust. *J. Neurosci.* **29**, 11783-11793.
- Held, M., Berz, A., Hensgen, R., Muenz, T. S., Scholl, C., Rössler, W., Homberg, U. and Pfeiffer, K. (2016). Microglomerular synaptic complexes in the sky-compass network of the honeybee connect parallel pathways from the anterior optic tubercle to the central complex. *Front. Behav. Neurosci.* **10**, 186.
- Hesselmann, G., Kell, C. A., Eger, E. and Kleinschmidt, A. (2008). Spontaneous local variations in ongoing neural activity bias perceptual decisions. *Proc. Natl. Acad. Sci. USA* **105**, 10984-10989.
- Homberg, U. and Müller, M. (2016). Ultrastructure of GABA- and tachykinin-immunoreactive neurons in the lower division of the central body of the desert locust. *Front. Behav. Neurosci.* **10**, 230.
- Homberg, U., Vitzthum, H., Müller, M. and Binkle, U. (1999). Immunocytochemistry of GABA in the central complex of the locust *Schistocerca gregaria*: identification of immunoreactive neurons and colocalization with neuropeptides. *J. Comp. Neurol.* **409**, 495-507.



- Homberg, U., Hofer, S., Pfeiffer, K. and Gebhardt, S.** (2003). Organization and neural connections of the anterior optic tubercle in the brain of the locust, *Schistocerca gregaria*. *J. Comp. Neurol.* **462**, 415-430.
- Homberg, U., Heinze, S., Pfeiffer, K., Kinoshita, M. and el Jundi, B.** (2011). Central neural coding of sky polarization in insects. *Philos. Trans. R. Soc. B* **366**, 680-687.
- Kennedy, J. S.** (1951). The migration of the desert locust (*Schistocerca gregaria* Forsk.). I. The behaviour of swarms. II. A theory of long-range migrations. *Philos. Trans. R. Soc. B* **235**, 163-290.
- Kim, S. S., Rouault, H., Druckmann, S. and Jayaraman, V.** (2017). Ring attractor dynamics in the *Drosophila* central brain. *Science* **356**, 849-853.
- Kinoshita, M., Pfeiffer, K. and Homberg, U.** (2007). Spectral properties of identified polarized-light sensitive interneurons in the brain of the desert locust *Schistocerca gregaria*. *J. Exp. Biol.* **210**, 1350-1361.
- Labhart, T. and Meyer, E. P.** (1999). Detectors for polarized skylight in insects: a survey of ommatidial specializations in the dorsal rim area of the compound eye. *Microsc. Res. Tech.* **47**, 368-379.
- Müller, M., Homberg, U. and Kühn, A.** (1997). Neuroarchitecture of the lower division of the central body in the brain of the locust (*Schistocerca gregaria*). *Cell Tissue Res.* **288**, 159-176.
- Neuser, K., Triphan, T., Mronz, M., Poeck, B. and Strauss, R.** (2008). Analysis of a spatial orientation memory in *Drosophila*. *Nature* **453**, 1244-1247.
- Ofstad, T. A., Zuker, C. S. and Reiser, M. B.** (2011). Visual place learning in *Drosophila melanogaster*. *Nature* **474**, 204-207.
- Omoto, J. J., Keleş, M. F., Nguyen, B.-C. M., Bolanos, C., Lovick, J. K., Frye, M. A. and Hartenstein, V.** (2017). Visual input to the *Drosophila* central complex by developmentally and functionally distinct neuronal populations. *Curr. Biol.* **27**, 1098-1110.
- Peters, B. H., Römer, H. and Marquart, V.** (1986). Spatial segregation of synaptic inputs and outputs in a locust auditory interneurone. *J. Comp. Neurol.* **254**, 34-50.
- Pfeiffer, K. and Homberg, U.** (2007). Coding of azimuthal directions via time-compensated combination of celestial compass cues. *Curr. Biol.* **17**, 960-965.
- Pfeiffer, K., Kinoshita, M. and Homberg, U.** (2005). Polarization-sensitive and light-sensitive neurons in two parallel pathways passing through the anterior optic tubercle in the locust brain. *J. Neurophysiol.* **94**, 3903-3915.
- Reppert, S. M., Zhu, H. and White, R. H.** (2004). Polarized light helps monarch butterflies navigate. *Curr. Biol.* **14**, 155-158.
- Rossel, S.** (1993). Navigation by bees using polarized skylight. *Comp. Biochem. Physiol. A* **104**, 695-708.
- Rossel, S., Wehner, R. and Lindauer, M.** (1978). E-vector orientation in bees. *J. Comp. Physiol. A* **125**, 1-12.
- Sakura, M., Lambrinos, D. and Labhart, T.** (2008). Polarized skylight navigation in insects: model and electrophysiology of e-vector coding by neurons in the central complex. *J. Neurophysiol.* **99**, 667-682.
- Seelig, J. D. and Jayaraman, V.** (2015). Neural dynamics for landmark orientation and angular path integration. *Nature* **521**, 186-191.
- Stalleicken, J., Mukhida, M., Labhart, T., Wehner, R., Frost, B. and Mouritsen, H.** (2005). Do monarch butterflies use polarized skylight for migratory orientation? *J. Exp. Biol.* **208**, 2399-2408.
- Taube, J. S. and Muller, R. U.** (1998). Comparisons of head direction cell activity in the postsubiculum and anterior thalamus of freely moving rats. *Hippocampus* **8**, 87-108.
- Träger, U. and Homberg, U.** (2011). Polarization-sensitive descending neurons in the locust: connecting the brain to thoracic ganglia. *J. Neurosci.* **31**, 2238-2247.
- Träger, U., Wagner, R., Bausenwein, B. and Homberg, U.** (2008). A novel type of microglomerular synaptic complex in the polarization vision pathway of the locust brain. *J. Comp. Neurol.* **506**, 288-300.
- Van der Meer, M. A. A., Knierim, J. J., Yoganarasimha, D., Wood, E. R. and van Rossum, M. C. W.** (2007). Anticipation in the rodent head direction system can be explained by an interaction of head movements and vestibular firing properties. *J. Neurophysiol.* **98**, 1883-1897.
- Varga, A. G. and Ritzmann, R. E.** (2016). Cellular basis of head direction and contextual cues in the insect brain. *Curr. Biol.* **26**, 1816-1828.
- von Frisch, K.** (1949). Die Polarisation des Himmelslichtes als orientierender Faktor bei den Tänzchen der Bienen. *Experientia* **5**, 142-148.
- Wehner, R.** (2001). Polarization vision – a uniform sensory capacity? *J. Exp. Biol.* **204**, 2589-2596.
- Wehner, R. and Müller, M.** (2006). The significance of direct sunlight and polarized skylight in the ant's celestial system of navigation. *Proc. Natl. Acad. Sci. USA* **103**, 12575-12579.
- Weir, P. T. and Dickinson, M. H.** (2012). Flying *Drosophila* orient to sky polarization. *Curr. Biol.* **22**, 21-27.
- Weir, P. T. and Dickinson, M. H.** (2015). Functional divisions for visual processing in the central brain of flying *Drosophila*. *Proc. Natl. Acad. Sci. USA* **112**, E5523-E5532.
- Wernet, M. F., Perry, M. W. and Desplan, C.** (2015). The evolutionary diversity of insect retinal mosaics: common design principles and emerging molecular logic. *Trends Genet.* **31**, 316-328.
- Zar, J. H.** (1999). *Biostatistical Analysis*, 4th edn. Upper Saddle River, NJ: Prentice Hall.

**Table S1: Responsiveness of central-complex neurons to the plane of polarized blue light and the azimuth of an unpolarized green and UV light spot.**  $n_{total}$ , total number of neurons;  $n_{sig.}$ , number of neurons with significant responses to all stimuli repetitions;  $n_{n.s.}$ , number of neurons that did not respond to any of the stimulus repetitions;  $N_{total}$ , total number of stimulus presentations;  $N_{sig.}$ , number of significant responses;  $\%N_{sig.}$ , percentage of significant responses.

<b>polarized blue</b>						
	$n_{total}$	$n_{sig.}$	$n_{n.s.}$	$N_{total}$	$N_{sig.}$	$\%N_{sig.}$
TL1	2	0	0	18	8	44
TL2	7	6	0	43	33	77
TL3	2	1	0	12	10	83
CL1	20	7	3	118	65	55
TB1	16	9	2	86	54	63
CPU1	19	4	2	130	84	65
CPU2	11	3	2	87	31	36
CP1	2	1	0	12	11	92
CP2	4	2	0	30	12	40
<b>unpolarized green</b>						
	$n_{total}$	$n_{sig.}$	$n_{n.s.}$	$N_{total}$	$N_{sig.}$	$\%N_{sig.}$
TL1	2	0	1	18	7	43
TL2	7	5	1	32	28	88
TL3	2	0	0	10	5	50
CL1	20	10	1	108	79	73
TB1	16	8	1	76	55	72
CPU1	19	10	2	113	79	70
CPU2	11	3	0	73	50	68
CP1	2	1	0	8	6	75
CP2	4	2	0	16	12	75
<b>unpolarized UV</b>						
	$n_{total}$	$n_{sig.}$	$n_{n.s.}$	$N_{total}$	$N_{sig.}$	$\%N_{sig.}$
TL1	2	0	1	8	1	12
TL2	7	5	1	24	18	75
TL3	2	0	0	8	3	38
CL1	18	10	2	60	44	73
TB1	10	5	3	36	20	56
CPU1	16	8	4	60	36	60
CPU2	8	4	0	26	20	77
CP1	2	0	0	6	2	33
CP2	4	0	0	14	6	43

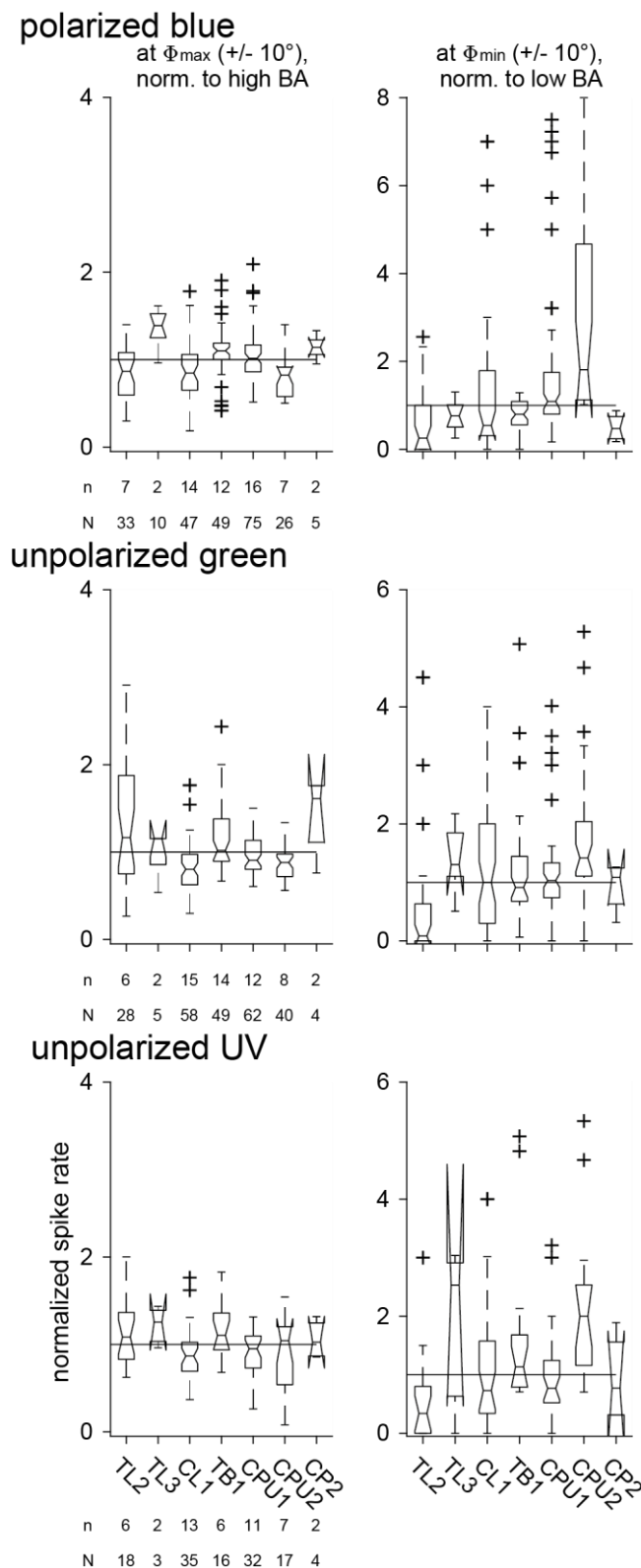


**Fig. S1. Effective amplitudes of tunings to the plane of polarized blue light and the azimuth of an unpolarized green and UV light spot.** Mean spiking activities at  $\Phi_{\max} \pm 10^\circ$  and  $\Phi_{\min} \pm 10^\circ$  are plotted from  $N$  responses of  $n$  neurons to polarized blue light, unpolarized green light, and unpolarized UV light. Spike rates are normalized to very high BA (the 97.5<sup>th</sup> percentile) or very low BA (the 2.5<sup>th</sup> percentile), respectively. Solid lines mark a value of 1. The upper limit of confidence interval exceeding unity in the left panels indicates excitation at  $\Phi_{\max}$ , the whole confidence interval exceeding unity indicates robust excitation at  $\Phi_{\max}$ . The lower limit of confidence interval undershooting unity in the right panels indicates inhibition at  $\Phi_{\min}$ , the whole confidence interval undershooting unity indicates robust inhibition at  $\Phi_{\min}$ .



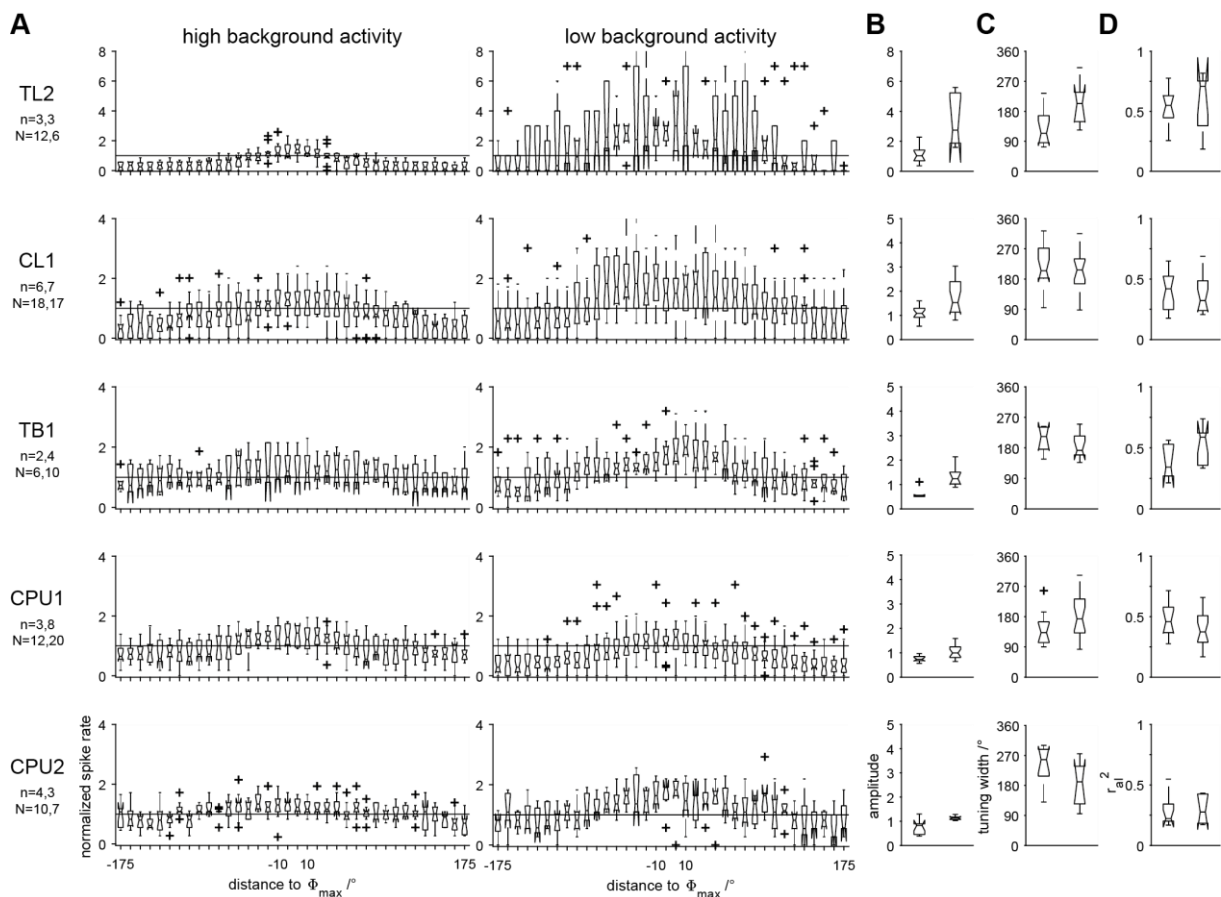


**Fig. S2. Comparison of tuning characteristics to unpolarized UV light during high and low background activity.** (A) Normalized stimulus response curves of  $N$  responses and  $n$  neurons to unpolarized UV light during high and low neuronal background activity. Spike angles (i.e. were shifted to  $\Phi_{\max}$  and binned in  $10^{\circ}$  wide bins. Stimulus response curves were normalized to the median neuronal BA (solid line at value 1). (B-D) Box plots showing amplitude, width and  $r_{al}^2$  of each response in (A) for each cell type during high and low BA.

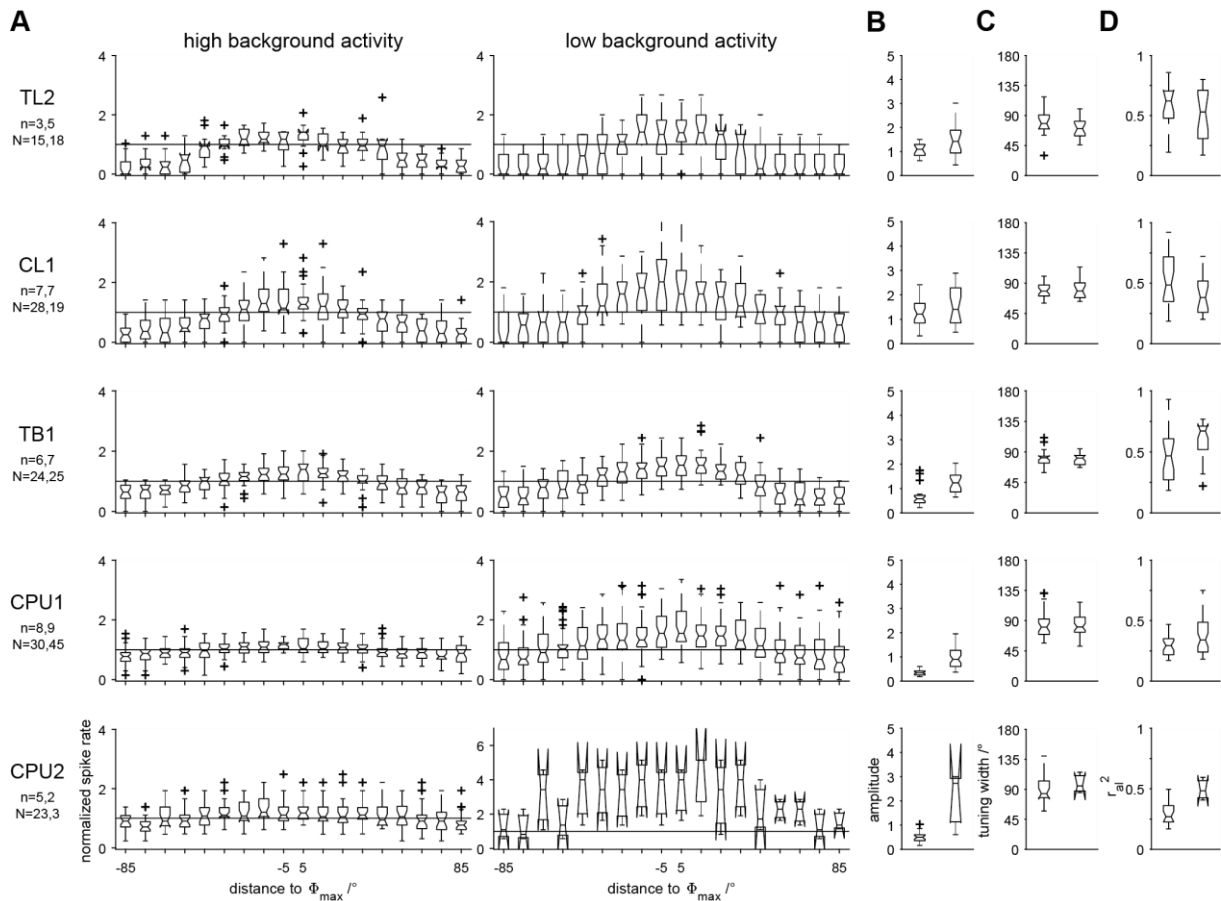


**Fig. S3. Comparison of tuning characteristics to polarized light during high and low background activity.** (A) Normalized stimulus response curves of  $N$  responses and  $n$  neurons to polarized blue light during high and low neuronal background activity. Spike angles were shifted to  $\Phi_{\max}$  and binned in  $10^{\circ}$  wide bins. Stimulus response curves were normalized to the median neuronal BA (solid line at value 1). (B-D) Box plots showing amplitude, width and  $r_{al}^2$  of each response in (A) for each cell type during high and low BA. Note that in (D)  $r_{al}^2$  of responses during high BA decreases from TL toward CPU2 neurons.

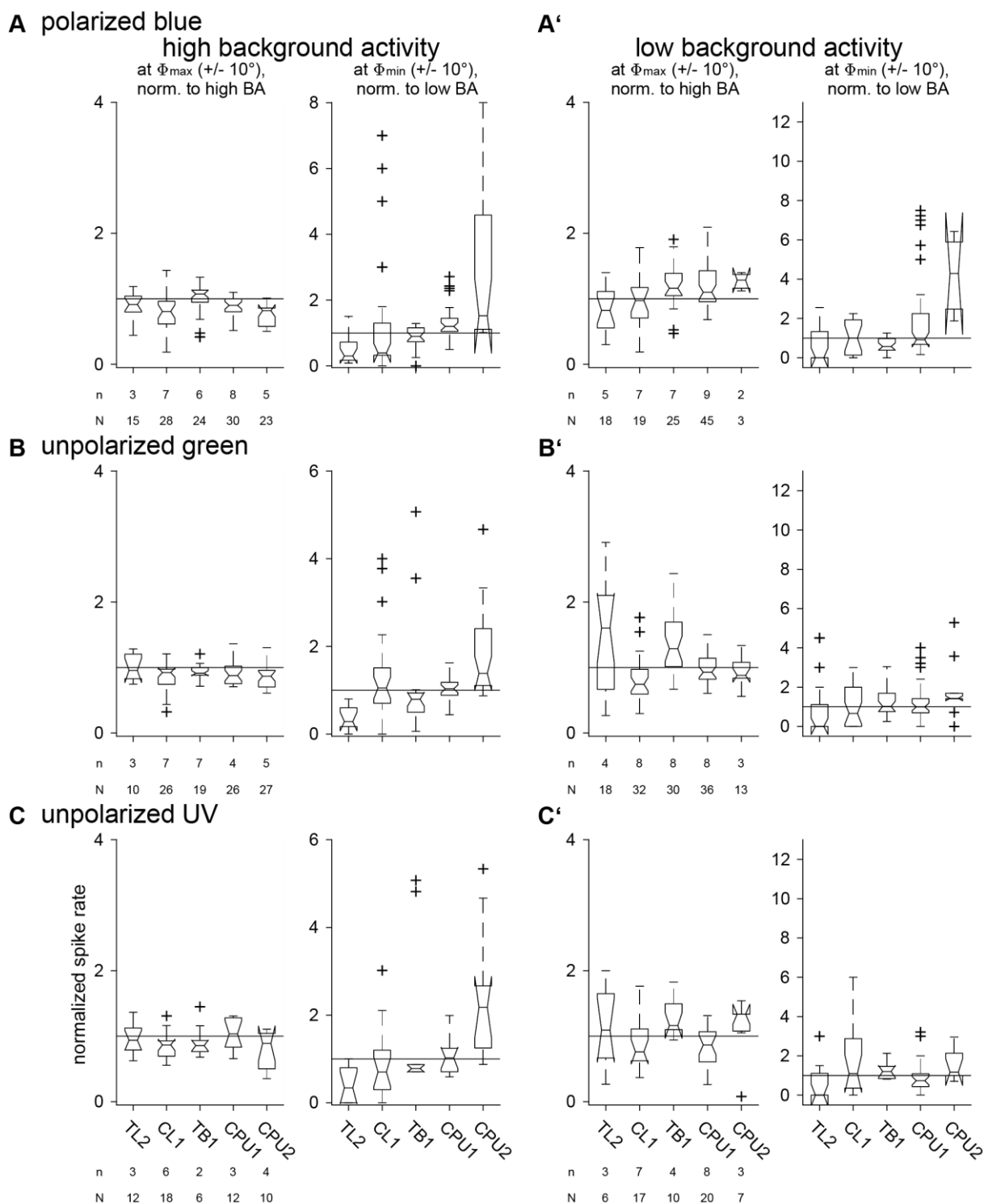


**Fig. S4. Comparison of effective amplitudes of responses to three different stimulation regimes in neurons with high and low background activity.** Mean spiking activities at  $\Phi_{\max} \pm 10^\circ$  and  $\Phi_{\min} \pm 10^\circ$  are plotted from  $N$  responses of  $n$  neurons to polarized blue light (A,A'), unpolarized green light (B,B'), and unpolarized UV light (C,C') during high and low BA. Spike rates were normalized to very high BA (i.e. the 97.5<sup>th</sup> percentile of BA), or very low BA (i.e. the 2.5<sup>th</sup> percentile of BA), respectively. Solid line marks a value of 1.

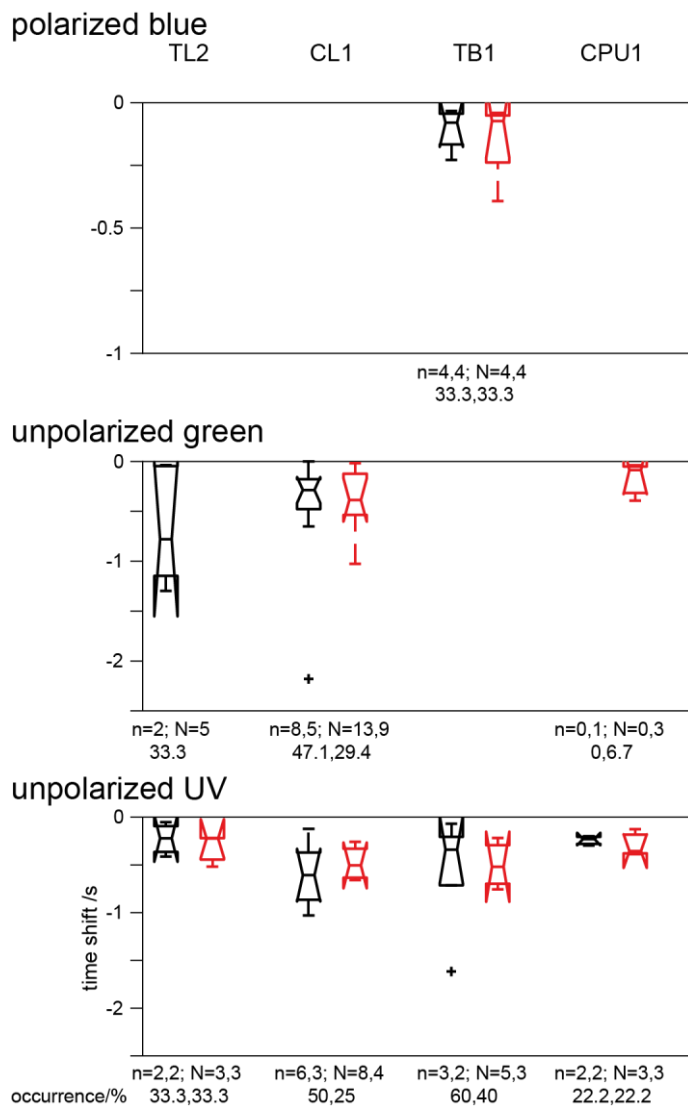


**Fig. S5. Response delays in responses to clockwise and counterclockwise stimulation.** Boxplots showing delays in  $\Phi_{\max}$  of individual responses to clockwise (black) and counterclockwise (red) rotations when compared to the pooled  $\Phi_{\max}$  of responses to all rotations.  $n$ , number of neurons,  $N$ , number of clockwise and counterclockwise rotations. Only cell types with  $N > 2$  are included. In recordings with different numbers of clockwise and counterclockwise responses, redundant responses were randomly excluded from analysis.